Czech Technical University in Prague
Faculty of Electrical Engineering
Department of Control Engineering

BACHELOR THESIS

Quadratic Programming Algorithms for Fast Model-Based Predictive Control

Prague, May 2013

Ondřej Mikuláš

Czech Technical University in Prague
Faculty of Electrical Engineering

Department of Control Engineering

BACHELOR PROJECT ASSIGNMENT

Student: **Ondřej Mikuláš**

Study programme: Cybernetics and Robotics
Specialisation: Systems and Control

Title of Bachelor Project: **QP algorithms for fast model-based predictive control**

Guidelines:

1. Using specific benchmark problems, evaluate the properties of selected algorithms of quadratic programming (QP) for fast Model Predictive Control (MPC) applications.
2. Select and justify suitable criteria to illustrate the distribution of computation time, control performance, and robustness of MPC controller as a function of problem size.

Bibliography/Sources:

[1] J. A. Rossiter, Model-Based Predictive Control: A Practical Approach. CRC Press, 2003.
[2] S. Boyd and L. Vandenberghe, Convex Optimization, vol. 98, no. 1. Cambridge University Press, 2004, p. 730.
[3] Y. Wang and S. Boyd, Fast model predictive control using online optimization, IEEE Transactions on Control Systems Technology, vol. 18, no. 2, pp. 267 - 278, 2010.
[4] H. J. Ferreau, H. G. Bock, and M. Diehl, An online active set strategy to overcome the limitations of explicit MPC, International Journal of Robust and Nonlinear Control, vol. 18, no. 8, pp. 816-830, 2008.
[5] S. Richter, C. N. Jones, and M. Morari, Real-time input-constrained MPC using fast gradient methods, in Proceedings of the 48th IEEE Conference on Decision and Control Conference, 2009, no. 1, pp. 7387-7393.

Bachelor Project Supervisor: Prof.Ing. Vladimír Havlena, CSc.

Valid until the summer semester 2013/2014

[illegible]

ČESKÉ VYSOKÉ UČENÍ TECHNICKÉ V PRAZE
Fakulta elektrotechnická
L.S.

[illegible]

prof. Ing. Michael Šebek, DrSc.
Head of Department

prof. Ing. Pavel Ripka, CSc.
Dean

Prague, January 24, 2013

Abstract

This thesis deals with quadratic programming (QP) algorithms for the use in fast model based predictive control applications. First, general overview of model based predictive control and quadratic programming is given. Then, several QP algorithms – active set method, fast gradient method and interior point method – are described.

Then, these algorithms are tested on model predictive control example and on randomly generated QPs. We treat especially computation time required to obtain a solution, the factors that influence the run-time (condition number, correction horizon etc.) and also the typical properties related to the computation time of the above mentioned algorithms.

Finally, the thesis deals with robust control performance of model predictive controller without constraints. With selected plants, the effect of plant model mismatch on the robust quality of control is studied in conjunction with correction horizon length.

Abstrakt

Tato práce se zabývá algoritmy kvadratického programování (QP) pro nasazení v rychlých aplikacích prediktivního řízení. Nejprve je podán obecný pohled na prediktivní řízení a kvadratické programování. Poté jsou představeny některé algoritmy QP – konkrétně metoda aktivních množin, rychlá gradientní metoda a metoda vnitřního bodu.

V další části jsou tyto algoritmy otestovány na příkladu prediktivní regulace a také pomocí náhodně generovaných QP. Důraz je kladen především na potřebnou dobou výpočtu a na to, jak je tato doba ovlivněna různými faktory (podmíněnost, korekční horizont a další) a jaké jsou typické vlastnosti uvedených algoritmů co se této doby týká.

Nakonec se práce věnuje robustnosti prediktivního regulátoru ve smyslu kvality řízení bez přítomnosti omezení. Na konkrétních soustavách popisuje vliv chybného modelu na kvalitu řízení v souvislosti s délkou korekčního horizontu.

Declaration

I hereby declare that I worked out the thesis individually and that I listed all the literature and software used.

In Prague on 24th May 2013, [illegible]

Ondřej Mikuláš

Acknowledgments

I would like to express many thanks to Vladimír Havlena for the supervision of my thesis and for the time he devoted to me. Next, many thanks come to Ondřej Šantin for many indispensable consultations. Last but not the least, let me thank to my family for their endless support during my studies.

Poděkování

Na tomto místě děkuji Vladimíru Havlenovi za vedení mé bakalářské práce a za čas který mi věnoval. Děkuji také Ondřeji Šantinovi za bezpočet konzultací, bez kterých by tato práce nebyla taková jaká je. Nakonec mi dovolte poděkovat mé rodině za jejich bezmeznou podporu v celém průběhu mého studia.

Contents

Chapter 1

Introduction

Model-based predictive control (MPC) is a modern, optimization driven control strategy. It involves a solution of an optimization problem at each time step. Therefore, fast optimization algorithms are required in order to control fast dynamic systems.

The objective of this thesis is to study the properties of quadratic programming (QP) algorithms that are suitable for the use in fast model predictive control applications. Another objective is to illustrate the influence of quadratic programming problem size on the control quality and robustness of model predictive controller.

The thesis is organized as follows. This chapter presents the basic idea of predictive control. Next, brief history overview is provided, and finally the state of the art is shown. The second chapter gives a more detailed description of MPC algorithm. The third chapter reviews optimization algorithms for QP problems. Namely gradient descent method and Newton's method for unconstrained QP, and active set method, fast gradient method and interior point method for inequality constrained QP.

The fourth chapter analyses the properties of the algorithms from the third chapter. Especially noted are the factors that influence the computation time. In the fifth chapter robustness of model predictive controller in terms of control quality is discussed.

1.1 Basic principle of predictive control

Predictive controllers use future system behavior *prediction* to choose an appropriate action. These controllers act a little bit like humans do. A person also predicts the consequence of his or her actions before doing one and usually chooses the best possible.

The prediction is made based on the model of the system and an actual state. So is the prediction made in our head. We also have to know how the system acts in different states. The need of the model is natural. When we come to some new situation, we should get some knowledge about it in order to be able to handle it.

At each time instant, a control action has to be selected, that results in the best predicted behavior. A *cost function* is defined to evaluate the cost of the predicted behavior. The cost function may reflect various things. From the difference between the actual behavior and the desired one (tracking error), to the costs of the control or to the violation of constraints put on the system. Then, a mathematical optimization problem is solved to obtain the control action that minimizes the cost function.

This control strategy is in contrast with classical control methods such as PID (proportional, integral, derivative). They do not make any adjustments based on the knowledge of the system and its future behavior. Typically, tracking error is measured and fed into the controller. An action is taken by PID only when an error occurs. On the other hand, predictive controller predicts that an error may occur in the future, so it takes an action at the moment to prevent it.

The following example is inspired by the one provided in [1]. Consider riding a motorbike. A skilled driver knows how the motorbike acts under various conditions (i.e. the model) and he also has some kind of cost function. Staying on the road is more important to him than going at high speed. Of course, different riders have different cost functions. When he approaches a sharp turn, he makes a prediction of his future trajectory at different speeds and directions. Then, he chooses the best of these actions based on their predicted cost. After that, he applies the correction and makes another prediction for the newly occurred situation. This repeats until the driver ends his route.

1.2 Brief history

Time to solve the underlying optimization problem had long restricted the use of MPC to slow dynamic processes. This includes various processes in petrochemical industry or chemical industry.

The first industrial applications date back to the late 1970's. We name for example Model predictive heuristic control in [2] or Dynamic matrix control in [3]. The earliest implementations of MPC used input/output models (impulse and step response) [4] because these models are readily available from experiments.

In the late 1980's Shell engineers introduced an implementation which made use of the state space process model. This package is called SMOC (Shell multivariable optimization controller) and it uses grey-box identification to obtain a plant model.

As the digital computers became faster and less expensive, the popularity of MPC grew. Today, it is a widely accepted and well known control method. Further history overview can be found in [5, sec. 2].

1.3 Predictive control at present

Today, various types of predictive control are referred to either as *predictive control* or as *model based predictive control.*

Increase in the computational power of hardware, new algorithms and intensive research has led to its wide spread. Even systems with fast dynamics that require short sampling times can be handled with today's algorithms and hardware.

MPC formulations can be divided according to norm used in a cost function. First, l_1 and l_∞ norms result in linear programming (LP). And second, l_2 or Euclidean norm results in quadratic programming (QP). We restrict our aim to the latter one only.

Significant results in QP algorithms specific to MPC have been reported in [6] (active set method), [7] (fast gradient method) or [8] (interior point method). These algorithms will be described in more detail in the following chapters.

Special attention is paid to the operation of MPC on inexpensive hardware (see e.g. [9]) or field-programmable gate arrays (for example [10]).

MPC is much appreciated for its ability to take system constraints (e.g. actuator limits) into account which makes it suitable for deployment in industrial process control. It is not restricted to systems with single input and single output and so even large scale multiple input multiple output (MIMO) systems can be controlled (for a survey of industrial applications see [5]). The design of a model based predictive controller for such a MIMO system is quite straightforward.

Notation

- $\mathbb{R}$ - set of real numbers
- Lower and upper case italic letters - scalars
- Bold lowercase letters $\mathbf{a}$ to $\mathbf{z}$ - column vectors in $\mathbb{R}^n$
- Bold uppercase letters $\mathbf{A}$ to $\mathbf{Z}$ - matrices in $\mathbb{R}^{m\times n}$
- $\mathbf{0}$ ($\mathbf{1}$) - vector or matrix of zeros (ones) of corresponding size
- $\mathbf{I}$ - identity matrix of corresponding size
- $\mathbf{A}^\mathrm{T}$ - matrix transpose

Chapter 2

Model based predictive control

This chapter presents more detailed description of model based predictive control algorithm for linear discrete-time systems. First, receding horizon principle is introduced, then prediction of future system states is shown. After that, the regulator and the tracking problems are described. Finally, specialized MPC formulation that allows offset-free tracking for nominal model with simple box constraints is presented. Great introductory text on MPC can be found e.g. in [1]. Note that in the following text, only state space models are considered.

2.1 Predictive control algorithm

Model based predictive controller makes a prediction of future system behavior based on its model, the current system state, the input trajectory, or a disturbance entering the system. Then, it selects the best possible input action according to a cost function. To do this it has to solve an optimization problem, subject to possible constraints. Finally, it applies the first element of the optimal selected input sequence to the system. At each time step, this procedure is repeated, which introduces so called receding horizon principle.

We describe these components in more detail in the following subsections.

2.1.1 Prediction

Prediction is a crucial part of a predictive controller. It is based on a model of a system to be controlled. For the prediction to be correct, the model has to be as exact as possible, as well as the state measurement or estimation. It enables the controller to predict consequence of its actions. The prediction is made only for a finite number of steps. This number is called *prediction horizon* and it is denoted as n_p.

Consider a linear time-invariant discrete-time model with n state variables in vector $\mathbf{x} \in \mathbb{R}^n$, m inputs in $\mathbf{u} \in \mathbb{R}^m$ and p outputs in $\mathbf{y} \in \mathbb{R}^p$. Its evolution is described by

$$\begin{aligned} \mathbf{x}_{k+1} &= \mathbf{A}\mathbf{x}_k + \mathbf{B}\mathbf{u}_k \\ \mathbf{y}_k &= \mathbf{C}\mathbf{x}_k + \mathbf{D}\mathbf{u}_k, \end{aligned} \tag{2.1}$$

where $\mathbf{A} \in \mathbb{R}^{n\times n}$, $\mathbf{B} \in \mathbb{R}^{n\times m}$, $\mathbf{C} \in \mathbb{R}^{p\times n}$ and $\mathbf{D} \in \mathbb{R}^{p\times m}$ are state space matrices. Now we write $\mathbf{x}_{k+2}$ in terms of $\mathbf{x}_{k+1}$ and $\mathbf{u}_{k+1}$ and then substitute from (2.1).

$$\begin{aligned} \mathbf{x}_{k+2} &= \mathbf{A}\mathbf{x}_{k+1} + \mathbf{B}\mathbf{u}_{k+1} = \mathbf{A}^2\mathbf{x}_k + \mathbf{A}\mathbf{B}\mathbf{u}_k + \mathbf{B}\mathbf{u}_{k+1}, \\ \mathbf{y}_{k+1} &= \mathbf{C}\mathbf{x}_{k+1} + \mathbf{D}\mathbf{u}_{k+1} = \mathbf{C}\mathbf{A}\mathbf{x}_k + \mathbf{C}\mathbf{B}\mathbf{u}_k + \mathbf{D}\mathbf{u}_{k+1}. \end{aligned} \tag{2.2}$$

Similar procedure can be done for the other future time steps. The resulting time series can be expressed in a convenient block matrix form. For the predicted system states we obtain the following:

$$\underbrace{\begin{bmatrix} \mathbf{x}_{k+1} \\ \mathbf{x}_{k+2} \\ \vdots \\ \mathbf{x}_{k+n_p} \end{bmatrix}}_{\mathbf{x}_{k+1,n_p}} = \underbrace{\begin{bmatrix} \mathbf{A} \\ \mathbf{A}^2 \\ \vdots \\ \mathbf{A}^{n_p} \end{bmatrix}}_{\mathbf{P}_x} \mathbf{x}_k + \underbrace{\begin{bmatrix} \mathbf{B} & \mathbf{0} & \cdots \\ \mathbf{A}\mathbf{B} & \mathbf{B} & \cdots \\ \vdots & \vdots & \ddots \\ \mathbf{A}^{n_p-1}\mathbf{B} & \mathbf{A}^{n_p-2}\mathbf{B} & \cdots \end{bmatrix}}_{\mathbf{H}_x} \underbrace{\begin{bmatrix} \mathbf{u}_k \\ \mathbf{u}_{k+1} \\ \vdots \\ \mathbf{u}_{k+n_p-1} \end{bmatrix}}_{\mathbf{u}_{k,n_p-1}}. \tag{2.3}$$

For the system outputs we get similar expression.

$$\underbrace{\begin{bmatrix} \mathbf{y}_k \\ \mathbf{y}_{k+1} \\ \mathbf{y}_{k+2} \\ \vdots \\ \mathbf{y}_{k+n_p-1} \end{bmatrix}}_{\mathbf{y}_{k,n_p-1}} = \underbrace{\begin{bmatrix} \mathbf{C} \\ \mathbf{C}\mathbf{A} \\ \mathbf{C}\mathbf{A}^2 \\ \vdots \\ \mathbf{C}\mathbf{A}^{n_p-1} \end{bmatrix}}_{\mathbf{P}} \mathbf{x}_k + \underbrace{\begin{bmatrix} \mathbf{D} & \mathbf{0} & \mathbf{0} & \cdots \\ \mathbf{C}\mathbf{B} & \mathbf{D} & \mathbf{0} & \cdots \\ \mathbf{C}\mathbf{A}\mathbf{B} & \mathbf{C}\mathbf{B} & \mathbf{D} & \cdots \\ \vdots & \vdots & \vdots & \ddots \\ \mathbf{C}\mathbf{A}^{n_p-2}\mathbf{B} & \mathbf{C}\mathbf{A}^{n_p-3}\mathbf{B} & \mathbf{C}\mathbf{A}^{n_p-4}B & \cdots \end{bmatrix}}_{\mathbf{H}} \mathbf{u}_{k,n_p-1}. \tag{2.4}$$

We call the matrices $\mathbf{P}_x$, $\mathbf{H}_x$, $\mathbf{P}$ and $\mathbf{H}$ *state* and *output prediction matrices* respectively. Obtaining a prediction of future system evolution is now straightforward. The only thing we need is an input time series $\mathbf{u}_{k,n_p-1}$ and an initial state vector $\mathbf{x}_k$. The prediction of system state and system output is now easily computed as

$$\mathbf{x}_{k+1,n_p} = \mathbf{P}_x\mathbf{x}_k + \mathbf{H}_x\mathbf{u}_{k,n_p-1} \quad \text{and} \quad \mathbf{y}_{k,n_p-1} = \mathbf{P}\mathbf{x}_k + \mathbf{H}\mathbf{u}_{k,n_p-1}. \tag{2.5}$$

2.1.2 Receding horizon

From the optimal input trajectory computed at a certain time step, only the first element is applied to the system. The rest is discarded. Then the system state is updated (measured or estimated) and a new prediction is made over the same number of steps n_p. This principle is called a *receding horizon* because the end of the interval is always moving towards the future.

One can ask what is the reason for applying only the first element of the optimal input trajectory. The input sequence is based on optimizing over the whole prediction horizon but only the first element of the sequence is based on actual measurement. The rest is based only on open-loop prediction [11, ch. 8].

Sometimes, only a certain number of steps $n_c < n_p$ is being manipulated during the optimization. The number n_c is called *correction horizon* or control horizon. After n_c

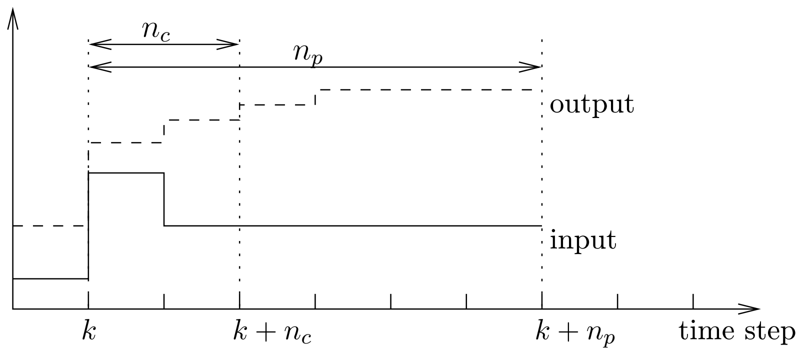

Figure 2.1: The concept of prediction and correction horizon and the receding horizon idea.

steps, the input is treated as unchanging. This is usually called *move blocking* and it will be discussed in more detail bellow. These concepts are illustrated in Figure 2.1.

2.1.3 Move blocking

The main reason for move blocking is the reduction of complexity of the optimization problem [1]. The number of degrees of freedom has major influence on the computation time.

Move blocking mentioned above is easily achieved using the following thought. We want the input to stay constant beyond the correction horizon n_c [1]. That is, to keep $\mathbf{u}_i = \mathbf{u}_{k+n_c-1}$ for all $i > k + n_c - 1$. This can be done by block matrix multiplication.

$$\mathbf{u}_{k,n_p-1} = \begin{bmatrix} \mathbf{u}_k \\ \vdots \\ \mathbf{u}_{k+n_c-1} \\ \vdots \\ \mathbf{u}_{k+n_p-1} \end{bmatrix} = \underbrace{\begin{bmatrix} \mathbf{I} & & \\ & \ddots & \\ & & \mathbf{I} \\ & & \vdots \\ & & \mathbf{I} \end{bmatrix}}_{\mathbf{M}_b} \underbrace{\begin{bmatrix} \mathbf{u}_k \\ \vdots \\ \mathbf{u}_{k+n_c-1} \end{bmatrix}}_{\mathbf{u}_{k,n_c-1}} . \tag{2.6}$$

Matrix $\mathbf{M}_b \in \mathbb{R}^{n_p m \times n_c m}$ can be either used together with input vector $\mathbf{u}_{k,n_c-1}$ ($\mathbf{u}_{k,n_p-1} = \mathbf{M}_b \mathbf{u}_{k,n_c-1}$) or modified prediction matrices $\mathbf{H}_{b,x}$ and $\mathbf{H}_b$ can be obtained.

$$\mathbf{H}_{b,x} = \mathbf{H}_x \mathbf{M}_b, \quad \mathbf{H}_b = \mathbf{H}\mathbf{M}_b \tag{2.7}$$

One can ask whether it is a good idea to put all the degrees of freedom to the start of the prediction horizon. There are various approaches to move blocking. For example, it is possible to spread the n_c allowed control moves evenly along the prediction horizon or to allow more moves in the beginning of the prediction horizon and less towards the end [12].

2.1.4 Cost function and optimization

A cost function gives us a way to assess the quality of predicted system output. It shows in a numerical way the predicted cost of certain input action.

For example consider a control system for house heating. The predicted cost should include the cost of the power needed to heat the house. It should include also a cost of the difference between the desired inside temperature and the predicted temperature. Of course, both things have different weight and it should be included as well. It is natural to select the action that minimizes the total predicted cost.

For the example above, we define a real valued cost function J in a similar way as in [1] to include a weighted sum of squared tracking errors $\mathbf{e}_i = \mathbf{y}_{r,i} - \mathbf{y}_i$ and inputs $\mathbf{u}_i$

$$J = \sum_{i=k}^{k+n_p-1} \mathbf{e}_i^{\mathrm{T}} \mathbf{Q}_i \mathbf{e}_i + \sum_{i=k}^{k+n_c-1} \mathbf{u}_i^{\mathrm{T}} \mathbf{R}_i \mathbf{u}_i, \tag{2.8}$$

with weighting matrices $\mathbf{Q}_i$ and $\mathbf{R}_i$ being positive semi-definite and positive definite respectively ($\mathbf{Q}_i \succeq 0$ and $\mathbf{R}_i \succ 0$) for all i. The definiteness is necessary for the resulting optimization problem to be convex as will be shown bellow.

These matrices allow us to put different costs to different outputs or inputs (elements of matrices) and even to different time steps (different matrix for different i).

At each time step, the cost function must be minimized in order to get the best possible input. The optimization can either be done on-line using a solver, or the optimal inputs can be precomputed off-line parametrized by the current system state.

Both ways have some drawbacks. On-line solution is restricted by the sampling time. The optimal solution has to be computed by the end of the sample. Otherwise, the input will not be well defined.

Off-line solution is also known as *explicit MPC* and it is described in [13]. The state space is divided into a number of convex regions, each of them corresponding to an affine-in-state control law. This approach is limited by possibly large number of the regions (exponential in the number of constraints). This fact puts great requirements on the memory storage.

2.1.5 Constraints

One of the major advantages of MPC over more conventional control methods is its ability to take constraints into account. There are two important classes of constraints.

Hard constraints These constraints are called hard, because it is impossible to violate them. They range from actuator limits to physically meaningful values such as non-negative applied braking force.

Soft constraints These are the constraints that can be violated at some cost, or under a penalty. They include for example economically viable setpoints or recommended temperature ranges.

Note that one should not use hard constraints on states or outputs, because it can lead to infeasibility. For example, a disturbance can affect the system such that it is not possible to satisfy all the hard constraints anymore. Thus, the optimization problem cannot be solved and the control action is undefined.

Constraints can be put also on the rate of change of the variables. For example, certain valve cannot be repositioned from 0 % to 100 % under 40 seconds.

Hard constraints

Consider for example upper and lower bounds on input variables. We want the inputs $\mathbf{u}_i$ to be less than or equal to some vector $\overline{\mathbf{u}}$ and greater than or equal to vector $\underline{\mathbf{u}}$. This should be true over the whole prediction horizon n_p. We can express it in compact matrix form $\mathbf{Su} \leq \mathbf{t}$. It is preferred over the other forms because it fits the notation used in mathematical optimization.

$$\underbrace{\begin{bmatrix} I & & \\ & \ddots & \\ & & I \\ -I & & \\ & \ddots & \\ & & -I \end{bmatrix}}_{\mathbf{S}\in\mathbb{R}^{2\cdot m\cdot n_p\times m\cdot n_p}} \mathbf{u}_{k,n_p-1} \leq \underbrace{\begin{bmatrix} \overline{\mathbf{u}} \\ \vdots \\ \overline{\mathbf{u}} \\ -\underline{\mathbf{u}} \\ \vdots \\ -\underline{\mathbf{u}} \end{bmatrix}}_{\mathbf{t}\in\mathbb{R}^{2\cdot m\cdot n_p\times 1}} . \tag{2.9}$$

Of course, these constraints can be put also on a subset of the prediction horizon. In a similar manner, constraints on the rate of change of inputs can be created. The only requirement is, that the constraints depend upon the variable over which the optimization happens, i.e. the input $\mathbf{u}$ or the input change $\Delta\mathbf{u}$. However, bound constraints on the inputs are the most common.

In order to use different constraints (e.g. input and rate of change of input limits) simultaneously, we just stack their matrices $\mathbf{S}$ and $\mathbf{t}$ from the expression $\mathbf{Su} \leq \mathbf{t}$ together.

These constraints are then put on the optimization problem and a solver has to take them into account. In the chapter devoted to quadratic programming, several algorithms employing constraints in this form will be presented.

Soft constraints

Soft constraints are the constraints that can be violated under some penalty or cost. In order to use them in predictive controller, we have to modify the cost function accordingly. It has to include the violation of soft constraints.

As an example, the construction of soft output upper bound will be shown. The basic idea is an introduction of a vector of *slack* variables $\mathbf{s}$. The vector is added to the output upper bound $\overline{\mathbf{y}}$ and the following inequality must hold.

$$\mathbf{y}_{k+1,n_p} \leq \overline{\mathbf{y}}_{k+1,n_p} + \mathbf{s}. \tag{2.10}$$

The predicted output vector is expressed in terms of prediction matrices (2.5) and

$$\mathbf{Px}_k + \mathbf{Hu}_{k,n_p-1} \leq \overline{\mathbf{y}}_{k+1,n_p} + \mathbf{s} \tag{2.11}$$

Then, the original cost function J is modified such that it penalizes $\mathbf{s}$. We have a new cost function with $\mathbf{Q}_s \succ 0$

$$J' = J + \sum_{i \in \mathcal{I}} \mathbf{s}^{\mathrm{T}} \mathbf{Q}_s \mathbf{s} \tag{2.12}$$

with new optimization variables in $\mathbf{s}$, that has to be minimized. Obviously, when $\mathbf{y}$ is less than or equal to the bound $\overline{\mathbf{y}}$, the minimizing $\mathbf{s}^{\star}$ is zero. Otherwise, the upper bound is violated but the amount of violation, expressed by $\mathbf{s}$, is penalized.

Note that the new variables in $\mathbf{s}$ increase the number of degrees of freedom in optimization. Hence, the soft constraints are usually included only to a modest number of steps, not over the whole prediction horizon.

More detailed description of soft constraints on outputs and states can be found e.g. in [14, sec. 2.3].

2.2 Regulator

In this section, we describe solution to the regulator problem. Optimal regulator should keep the system state in the origin, i.e. the operating point. That is, minimize a cost function that includes a weighted sum of squared state and input variables over the prediction horizon. We denote it J and define it as follows:

$$J = \frac{1}{2} \left(\sum_{i=k+1}^{k+n_p} \mathbf{x}_i^{\mathrm{T}} \mathbf{Q}_i \mathbf{x}_i + \sum_{i=k}^{k+n_c-1} \mathbf{u}_i^{\mathrm{T}} \mathbf{R}_i \mathbf{u}_i \right). \tag{2.13}$$

Predicted states $\mathbf{x}_i$ can be expressed using prediction matrices from (2.3) (with move blocking from (2.7)) using initial state vector $\mathbf{x}_k$ and input trajectory $\mathbf{u}_{k,n_c-1}$ only. Weighting matrices $\mathbf{Q}_i \in \mathbb{R}^{n \times n}$, $\mathbf{Q}_i \succeq 0$ and $\mathbf{R}_i \in \mathbb{R}^{m \times m}$, $\mathbf{R}_i \succ 0$ form new block diagonal matrices $\mathbf{Q}' \in \mathbb{R}^{n \cdot n_p \times n \cdot n_p}$ and $\mathbf{R}' \in \mathbb{R}^{m \cdot n_c \times m \cdot n_c}$ with the same definiteness. In order to keep the formulas short, we denote input trajectory $\mathbf{u}_{k,n_c-1}$ simply as $\mathbf{u}$.

$$J = \frac{1}{2} \left((\mathbf{P}_x \mathbf{x}_k + \mathbf{H}_{b,x} \mathbf{u})^{\mathrm{T}} \mathbf{Q}' (\mathbf{P}_x \mathbf{x}_k + \mathbf{H}_{b,x} \mathbf{u}) + \mathbf{u}^{\mathrm{T}} \mathbf{R}' \mathbf{u} \right) \tag{2.14}$$

After basic algebraic manipulation (multiplication and factoring out $\mathbf{u}$) we obtain

$$J = \frac{1}{2} \mathbf{u}^{\mathrm{T}} \underbrace{(\mathbf{H}_{b,x}^{\mathrm{T}} \mathbf{Q}' \mathbf{H}_{b,x} + \mathbf{R}')}_{\mathbf{G}} \mathbf{u} + \underbrace{(\mathbf{x}_k^{\mathrm{T}} \mathbf{P}_x^{\mathrm{T}} \mathbf{Q}' \mathbf{H}_{b,x})}_{\mathbf{f}^{\mathrm{T}}} \mathbf{u} + \underbrace{\mathbf{x}_k^{\mathrm{T}} (\mathbf{P}_x \mathbf{Q}' \mathbf{P}_x) \mathbf{x}_k}_{c}. \tag{2.15}$$

We denote the terms in (2.15) $\mathbf{G} \in \mathbb{R}^{m \cdot n_c \times m \cdot n_c}$, $\mathbf{f}^{\mathrm{T}} \in \mathbb{R}^{m \cdot n_c}$ and $c \in \mathbb{R}$. It can be readily shown, that $\mathbf{G}$ is positive definite[1]. Note the last term c which does not depend on $\mathbf{u}$ and so it is constant for fixed $\mathbf{x}_k$. The regulator problem can now be restated as an

[1]For all $\mathbf{x} \neq \mathbf{0}$ the following inequality holds. $\mathbf{x}^{\mathrm{T}}(\mathbf{H}_{b,x}^{\mathrm{T}} \mathbf{Q}' \mathbf{H}_{b,x} + \mathbf{R}')\mathbf{x} = \underbrace{\mathbf{x}^{\mathrm{T}}(\mathbf{H}_{b,x}^{\mathrm{T}} \mathbf{Q}' \mathbf{H}_{b,x})\mathbf{x}}_{\geq 0} + \underbrace{\mathbf{x}^{\mathrm{T}} \mathbf{R}' \mathbf{x}}_{>0} > 0$, since $\mathbf{Q}' \succeq 0$ and $\mathbf{R}' \succ 0$. Hence, $\mathbf{G}$ in (2.15) is positive definite.

optimization problem

$$\begin{aligned} &\text{minimize} && \frac{1}{2}\mathbf{u}^{\mathrm{T}}\mathbf{G}\mathbf{u} + \mathbf{f}^{\mathrm{T}}\mathbf{u} + c \\ &\text{subject to} && \text{constraints on } \mathbf{u}. \end{aligned} \tag{2.16}$$

In case of affine constraints, this optimization problem is a quadratic program but we deffer the definition until the next chapter.

2.3 Reference tracking

In this section, tracking of piecewise constant references for outputs will be discussed. First, state space model has to be augmented in order to include the references. Then, tracking error can be calculated and used in the cost function simply.

2.3.1 State space model to include references

In order to take tracking error into account, output reference has to be added to the model. To do this, a new state vector $\mathbf{y}_r \in \mathbb{R}^p$ will be stacked to the existing one. The reference states can have various dynamics but throughout this work, we assume them to be independent of the inputs and to be constant over the whole prediction horizon. That is

$$\underbrace{\begin{bmatrix} \mathbf{x}_{k+1} \\ \mathbf{y}_{r,k+1} \end{bmatrix}}_{\tilde{\mathbf{x}}_{k+1}} = \underbrace{\begin{bmatrix} \mathbf{A} & \mathbf{0} \\ \mathbf{0} & \mathbf{I} \end{bmatrix}}_{\tilde{\mathbf{A}}} \underbrace{\begin{bmatrix} \mathbf{x}_{k} \\ \mathbf{y}_{r,k} \end{bmatrix}}_{\tilde{\mathbf{x}}_{k}} + \underbrace{\begin{bmatrix} \mathbf{B} \\ \mathbf{0} \end{bmatrix}}_{\tilde{\mathbf{B}}} \mathbf{u}_k. \tag{2.17}$$

This equation introduces the extended state vector $\tilde{\mathbf{x}}$ together with state space matrices $\tilde{\mathbf{A}}$ and $\tilde{\mathbf{B}}$.

2.3.2 Output and tracking error

The output of this augmented model is exactly the same as the one of the original model (2.1) and it is given by

$$\mathbf{y}_k = \underbrace{\begin{bmatrix} \mathbf{C} & \mathbf{0} \end{bmatrix}}_{\tilde{\mathbf{C}}} \tilde{\mathbf{x}}_k + \mathbf{D}\mathbf{u}_k. \tag{2.18}$$

The tracking error is easily obtained from the augmented state space model. The reference has to be subtracted from the actual output, that is

$$\mathbf{e}_k = \underbrace{\begin{bmatrix} \mathbf{C} & -\mathbf{I} \end{bmatrix}}_{\tilde{\mathbf{C}}_e} \tilde{\mathbf{x}}_k + \mathbf{D}\mathbf{u}_k. \tag{2.19}$$

Prediction matrices for the tracking error $\tilde{\mathbf{P}}$ and $\tilde{\mathbf{H}}_b$ can be constructed according to Equations (2.4) and (2.7) with the only difference being the use of matrices $\tilde{\mathbf{A}}$, $\tilde{\mathbf{B}}$ and $\tilde{\mathbf{C}}_e$ instead of the original ones, so we refer there. Predicted errors are given as in (2.5) by

$$\mathbf{e}_{k,n_p-1} = \tilde{\mathbf{P}}\tilde{\mathbf{x}}_{\mathbf{k}} + \tilde{\mathbf{H}}_b\mathbf{u}, \tag{2.20}$$

where $\mathbf{u}$ is a shorthand denoting the input trajectory $\mathbf{u}_{k,n_c-1}$ as in the previous section.

2.3.3 Cost function

The cost function can be stated as a weighted sum of squared tracking errors and squared control inputs.

$$J = \frac{1}{2}\left(\sum_{i=k}^{k+n_p-1} \mathbf{e}_i^{\mathrm{T}}\mathbf{Q}_i\mathbf{e}_i + \sum_{i=k}^{k+n_c-1} \mathbf{u}_i^{\mathrm{T}}\mathbf{R}_i\mathbf{u}_i\right), \tag{2.21}$$

with symmetric matrices $\mathbf{Q}_i \in \mathbb{R}^{p\times p}$ ($\mathbf{Q}_i \succeq 0$) and $\mathbf{R}_i \in \mathbb{R}^{m\times m}$ ($\mathbf{R}_i \succ 0$). This function can now be expressed in terms of predicted error variables (2.20). The same simplification as in the previous section yields the result

$$J = \frac{1}{2}\mathbf{u}^{\mathrm{T}}\underbrace{(\tilde{\mathbf{H}}_b^{\mathrm{T}}\mathbf{Q}'\tilde{\mathbf{H}}_b + \mathbf{R}')}_{\mathbf{G}}\mathbf{u} + \underbrace{(\tilde{\mathbf{x}}_k^{\mathrm{T}}\tilde{\mathbf{P}}_x^{\mathrm{T}}\mathbf{Q}'\tilde{\mathbf{H}}_b)}_{\mathbf{f}^{\mathrm{T}}}\mathbf{u} + \underbrace{\tilde{\mathbf{x}}_k^{\mathrm{T}}(\tilde{\mathbf{P}}_x\mathbf{Q}'\tilde{\mathbf{P}}_x)\tilde{\mathbf{x}}_k}_{c}. \tag{2.22}$$

Matrix $\mathbf{G}$ is positive definite, for the same reason as in (2.15). Finally, an optimization problem in the same form as in (2.16) arises. The predictive controller has to solve the following optimization problem at each time instant.

$$\begin{aligned} &\text{minimize} && \frac{1}{2}\mathbf{u}^{\mathrm{T}}\mathbf{G}\mathbf{u} + \mathbf{f}^{\mathrm{T}}\mathbf{u} + c \\ &\text{subject to} && \text{constraints on } \mathbf{u}. \end{aligned} \tag{2.23}$$

2.4 Offset-free tracking

In order to ensure offset-free tracking for the nominal system and piecewise constant references, the control has to be unchanging in the steady state, when the model is exact. Thus, it is convenient to introduce so called *incremental formulation* of MPC.

The cost function has to be modified in a way that the following applies [1]. In steady state, the optimal value of the cost function J must correspond to zero tracking error $\mathbf{e}_{ss} \to 0$. Once this condition is met, the optimal input change $\Delta\mathbf{u}_{ss}$ must be zero, that is, the prediction must be unbiased.

For a reason that will become evident in the next chapter, we present a modified version of this formulation that penalizes the input changes $\Delta\mathbf{u}_i = \mathbf{u}_i - \mathbf{u}_{i-1}$ (also control increments) but optimizes over $\mathbf{u}$. It allows one to preserve simple lower and upper bound constraints on input variables. If the optimization happened over $\Delta\mathbf{u}$ the constraints on inputs would be far more complicated.

First, we introduce augmented state space model that includes references $\mathbf{y}_r$ for outputs (constant over the prediction horizon) and previous input vector $\mathbf{u}_{-1}$ (which is constant as well). It is described by the following equation.

$$\underbrace{\begin{bmatrix} \mathbf{x}_{k+1} \\ \mathbf{y}_{r,k+1} \\ \mathbf{u}_{-1} \end{bmatrix}}_{\hat{\mathbf{x}}_{k+1}} = \underbrace{\begin{bmatrix} \mathbf{A} & \mathbf{0} & \mathbf{0} \\ \mathbf{0} & \mathbf{I} & \mathbf{0} \\ \mathbf{0} & \mathbf{0} & \mathbf{I} \end{bmatrix}}_{\hat{\mathbf{A}}} \underbrace{\begin{bmatrix} \mathbf{x}_{k} \\ \mathbf{y}_{r,k} \\ \mathbf{u}_{-1} \end{bmatrix}}_{\hat{\mathbf{x}}_{k}} + \underbrace{\begin{bmatrix} \mathbf{B} \\ \mathbf{0} \\ \mathbf{0} \end{bmatrix}}_{\hat{\mathbf{B}}} \mathbf{u}_k. \tag{2.24}$$

In order to calculate the tracking error $\mathbf{e}$, the reference has to be subtracted from the output. While introducing a new matrix $\hat{\mathbf{C}}_e$, it is given by the following expression.

$$\mathbf{e}_k = \underbrace{\begin{bmatrix} \mathbf{C} & -\mathbf{I} & \mathbf{0} \end{bmatrix}}_{\hat{\mathbf{C}}_e} \hat{\mathbf{x}}_k + \mathbf{D}\mathbf{u}_k. \tag{2.25}$$

Prediction matrices $\hat{\mathbf{P}}$ and $\hat{\mathbf{H}}_b$ for the tracking error are derived in exactly the same manner as in (2.4) and (2.7) with matrices $\hat{\mathbf{A}}$, $\hat{\mathbf{B}}$, $\hat{\mathbf{C}}_e$ and $\mathbf{D}$. Prediction of the future error evolution is given by

$$\mathbf{e}_{k,n_p-1} = \hat{\mathbf{P}}\hat{\mathbf{x}}_k + \hat{\mathbf{H}}_b\mathbf{u}_{k,n_c-1}. \tag{2.26}$$

Now we express the input change $\Delta\mathbf{u}_i = \mathbf{u}_i - \mathbf{u}_{i-1}$ for the whole prediction horizon in matrix form. In addition, the previous input $\mathbf{u}_{k-1}$ has to be subtracted from the current input $\mathbf{u}_k$.

$$\underbrace{\begin{bmatrix} \Delta\mathbf{u}_k \\ \Delta\mathbf{u}_{k+1} \\ \Delta\mathbf{u}_{k+2} \\ \vdots \end{bmatrix}}_{\Delta\mathbf{u}_{k,n_c-1}} = \underbrace{\begin{bmatrix} \mathbf{I} & \mathbf{0} & \mathbf{0} & \cdots \\ -\mathbf{I} & \mathbf{I} & \mathbf{0} & \cdots \\ \mathbf{0} & -\mathbf{I} & \mathbf{I} & \\ \vdots & & \ddots & \ddots \end{bmatrix}}_{\mathbf{K}\in\mathbb{R}^{m\cdot n_c\times m\cdot n_c}} \underbrace{\begin{bmatrix} \mathbf{u}_k \\ \mathbf{u}_{k+1} \\ \mathbf{u}_{k+2} \\ \vdots \end{bmatrix}}_{\mathbf{u}_{k,n_c-1}} + \underbrace{\begin{bmatrix} -\mathbf{I} \\ \mathbf{0} \\ \mathbf{0} \\ \vdots \end{bmatrix}}_{\mathbf{M}} \mathbf{u}_{k-1}. \tag{2.27}$$

The last term $\mathbf{u}_{k-1}$ is easily obtained from the current state vector $\hat{\mathbf{x}}_k$ as

$$\mathbf{u}_{k-1} = \underbrace{\begin{bmatrix} \mathbf{0} & \mathbf{0} & \mathbf{I} \end{bmatrix}}_{\mathbf{L}} \hat{\mathbf{x}}_k. \tag{2.28}$$

We define the cost function that penalizes control changes $\Delta\mathbf{u}$ and tracking errors $\mathbf{e}$ with symmetric matrices $\mathbf{Q}_i \in \mathbb{R}^{p\times p}$ ($\mathbf{Q}_i \succeq 0$) and $\mathbf{R}_i \in \mathbb{R}^{m\times m}$ ($\mathbf{R}_i \succ 0$) by the following expression:

$$\begin{aligned} J &= \frac{1}{2}\left(\sum_{i=k}^{k+n_p-1} \mathbf{e}_i^{\mathrm{T}}\mathbf{Q}_i\mathbf{e}_i + \sum_{i=k}^{k+n_c-1} \Delta\mathbf{u}_i^{\mathrm{T}}\mathbf{R}_i\Delta\mathbf{u}_i\right) \\ &= \frac{1}{2}\left(\mathbf{e}_{k,n_p-1}^{\mathrm{T}}\mathbf{Q}'\mathbf{e}_{k,n_p-1} + \Delta\mathbf{u}_{k,n_c-1}^{\mathrm{T}}\mathbf{R}'\Delta\mathbf{u}_{k,n_c-1}\right). \end{aligned} \tag{2.29}$$

Afterwards, we substitute from (2.26), (2.27), and for notational convenience we mark $\mathbf{u}_{k,n_c-1}$ as $\mathbf{u}$ to obtain

$$\begin{aligned} J = &\frac{1}{2}(\hat{\mathbf{P}}\hat{\mathbf{x}}_k + \hat{\mathbf{H}}_b\mathbf{u})^{\mathrm{T}}\mathbf{Q}'(\hat{\mathbf{P}}\hat{\mathbf{x}}_k + \hat{\mathbf{H}}_b\mathbf{u}) \\ &+\frac{1}{2}(\mathbf{K}\mathbf{u} + \mathbf{M}\mathbf{L}\hat{\mathbf{x}}_k)^{\mathrm{T}}\mathbf{R}'(\mathbf{K}\mathbf{u} + \mathbf{M}\mathbf{L}\hat{\mathbf{x}}_k). \end{aligned} \tag{2.30}$$

Then we expand it and simplify to obtain a quadratic function in the form

$$J = \frac{1}{2}\mathbf{u}^{\mathrm{T}}\mathbf{G}\mathbf{u} + \mathbf{f}^{\mathrm{T}}\mathbf{u} + c, \tag{2.31}$$

where

$$\begin{aligned} \mathbf{G} &= \hat{\mathbf{H}}_b^{\mathrm{T}}\mathbf{Q}'\hat{\mathbf{H}}_b + \mathbf{K}^{\mathrm{T}}\mathbf{R}'\mathbf{K} \\ \mathbf{f}^{\mathrm{T}} &= \hat{\mathbf{x}}_k^{\mathrm{T}}(\hat{\mathbf{P}}^{\mathrm{T}}\mathbf{Q}'\hat{\mathbf{H}}_b + \mathbf{L}^{\mathrm{T}}\mathbf{M}^{\mathrm{T}}\mathbf{R}'\mathbf{K}) \\ c &= \frac{1}{2}\hat{\mathbf{x}}_k^{\mathrm{T}}(\hat{\mathbf{P}}^{\mathrm{T}}\mathbf{Q}'\hat{\mathbf{P}} + \mathbf{L}^{\mathrm{T}}\mathbf{M}^{\mathrm{T}}\mathbf{R}'\mathbf{M}\mathbf{L})\hat{\mathbf{x}}_k. \end{aligned} \tag{2.32}$$

Note that because $\mathbf{K}$ clearly has trivial kernel, only zero vector maps to zero vector. Therefore $\mathbf{G}$ is positive definite.

Minimization of this cost function is a quadratic program

$$\begin{aligned} &\text{minimize} && \frac{1}{2}\mathbf{u}^{\mathrm{T}}\mathbf{G}\mathbf{u} + \mathbf{f}^{\mathrm{T}}\mathbf{u} + c \\ &\text{subject to} && \text{constraints on } \mathbf{u}, \end{aligned} \tag{2.33}$$

which has to be solved at each time step.

2.5 Unconstrained MPC

In this section, it will be shown that if there are no constraints present, the predictive control law reduces to static state feedback controller. This fact enables one to study the closed loop dynamics using traditional techniques such as poles and zeros analysis, or frequency domain analysis.

We solve only the case from Section 2.4 but the others are analogous. Let us start with the optimization problem (2.33) but with no constraints. Note that the solution of quadratic programs will be thoroughly discussed in the following chapter.

The optimality condition requires the gradient of the objective function to equal zero vector. That is $\mathbf{G}\mathbf{u} + \mathbf{f} = \mathbf{0}$, and thus $\mathbf{u} = -\mathbf{G}^{-1}\mathbf{f}$. Please note that more efficient method to solve this system involves Cholesky factorization and it is described thoroughly in Section 3.3.

In order to get the current input, we have to select only the first block of optimal trajectory. This is achieved by the following operation:

$$\mathbf{u}_k = -\mathbf{N}\mathbf{G}^{-1}\mathbf{f}, \quad \text{where} \quad \mathbf{N} = \begin{bmatrix} \mathbf{I} & \mathbf{0} & \cdots & \mathbf{0} \end{bmatrix} \in \mathbb{R}^{m \times m \cdot n_c}. \tag{2.34}$$

Furthermore, $\mathbf{f}$ is a multiple of the augmented state vector $\hat{\mathbf{x}}_k$ as can be seen in (2.32). It immediately follows that

$$\mathbf{u}_k = -\underbrace{\mathbf{N}(\hat{\mathbf{H}}_b^{\mathrm{T}}\mathbf{Q}'\hat{\mathbf{H}}_b + \mathbf{K}^{\mathrm{T}}\mathbf{R}'\mathbf{K})^{-1}(\hat{\mathbf{H}}_b^{\mathrm{T}}\mathbf{Q}'\hat{\mathbf{P}} + \mathbf{K}^{\mathrm{T}}\mathbf{R}'\mathbf{L}\mathbf{M})}_{\mathbf{Z}}\hat{\mathbf{x}}_k. \tag{2.35}$$

We can divide $\mathbf{Z} \in \mathbb{R}^{m \times (n+p+m)}$ into three submatrices $\mathbf{Z}_1$, $\mathbf{Z}_2$ and $\mathbf{Z}_3$ according to the blocks of $\hat{\mathbf{x}}_k$ (it is defined in (2.24)) as follows:

$$\mathbf{u}_k = -\underbrace{\begin{bmatrix}\mathbf{Z}_1 & \mathbf{Z}_2 & \mathbf{Z}_3\end{bmatrix}}_{\mathbf{Z}}\underbrace{\begin{bmatrix}\mathbf{x}_k \\ \mathbf{y}_{r,k} \\ \mathbf{u}_{-1}\end{bmatrix}}_{\hat{\mathbf{x}}_k}. \tag{2.36}$$

Therefore, the resulting control law is a simple state feedback with matrix $\mathbf{Z}_1$ together with output reference ($\mathbf{Z}_2$) and last input ($\mathbf{Z}_3$) feedforward. The resulting closed loop poles are the eigenvalues of matrix $\mathbf{A} - \mathbf{B}\mathbf{Z}_1$ (see e.g. [15]).

Chapter 3

Quadratic programming algorithms

In the beginning of this chapter we define a quadratic program and state conditions for a quadratic program to be convex. Then we divide the programs into three classes according to the type of constraints they include. Finally, basic algorithms to solve each class of quadratic programs will be presented.

3.1 Quadratic programming

Let $\mathbf{G} \in \mathbb{R}^{n\times n}$ be a symmetric matrix ($\mathbf{G} = \mathbf{G}^{\mathrm{T}}$), $\mathbf{f} \in \mathbb{R}^n$ be a column vector and $c \in \mathbb{R}$ be a constant. We say that $q : \mathbb{R}^n \to \mathbb{R}$, written as

$$q(\mathbf{x}) = \frac{1}{2}\mathbf{x}^{\mathrm{T}}\mathbf{G}\mathbf{x} + \mathbf{f}^{\mathrm{T}}\mathbf{x} + c, \tag{3.1}$$

is a *quadratic function* if $\mathbf{G} \neq \mathbf{0}$. If $\mathbf{G}$ is a zero matrix, then q is an *affine function.*

We state form of Jacobian and Hessian matrices and gradient respectively, because we will refer to them often in the following sections.

$$q'(\mathbf{x}) = \mathbf{x}^{\mathrm{T}}\mathbf{G} + \mathbf{f}^{\mathrm{T}}, \qquad q''(\mathbf{x}) = \mathbf{G}, \qquad \nabla q(\mathbf{x}) = \mathbf{G}\mathbf{x} + \mathbf{f} = q'(\mathbf{x})^{\mathrm{T}} \tag{3.2}$$

3.1.1 Quadratic program

Minimization of a quadratic function under affine constraints is called a *quadratic program* (QP). Often, only the minimizer $\mathbf{x}^\star$ is of interest and so the constant term c is left out because it has no effect on $\mathbf{x}^\star$. A quadratic program can be written as follows:

$$\begin{aligned} \text{minimize} \quad & \frac{1}{2}\mathbf{x}^{\mathrm{T}}\mathbf{G}\mathbf{x} + \mathbf{f}^{\mathrm{T}}\mathbf{x} \\ \text{subject to} \quad & \mathbf{A}\mathbf{x} \leq \mathbf{b} \\ & \mathbf{A}_e\mathbf{x} = \mathbf{b}_e, \end{aligned} \tag{3.3}$$

where $\mathbf{A} \in \mathbb{R}^{m\times n}$ with column vector $\mathbf{b} \in \mathbb{R}^m$ and $\mathbf{A}_e \in \mathbb{R}^{l\times n}$ with $\mathbf{b}_e \in \mathbb{R}^l$ define a *feasible set.* The feasible set is an intersection of half-spaces (given by inequality constraints) and hyperplanes (given by equality constraints). Intersection of a finite number of half-spaces is called a *polytope*. Detailed information on polytopes can be found e.g. in [16].

Depending on the definiteness of Hessian matrix $q''(\mathbf{x}) = \mathbf{G}$ one of the following cases occurs:

G positive semidefinite: problem (3.3) is convex and thus every local minimizer is a global minimizer. Proof to be found in [17].

G positive definite: problem (3.3) is strictly convex and $\mathbf{G}$ is guaranteed to have full rank. The statement about local optima being globally optimal holds as with positive semidefinite $\mathbf{G}$. Moreover, the global minimizer is unique. Note that in model predictive control, quadratic programs are exclusively constructed such that this case occurs. Hence, in the following we assume that $\mathbf{G} \succ \mathbf{0}$.

G negative semidefinite: problem (3.3) is concave. Minimum is attained at the boundary of a feasible set. Different algorithms have to be used to find global minimum. It is not the subject of this thesis.

G negative definite: special case of negative semidefinite Hessian matrix except that $\mathbf{G}$ has full rank. The same comments apply.

G indefinite: problem (3.3) is non-convex, so a global solver has to be used to find the global minimum, which is far more complicated.

3.2 KKT optimality conditions

First order optimality conditions for nonlinear optimization problems are called *Karush-Kuhn-Tucker* (KKT) conditions. These conditions are necessary, in special cases (e.g. convex optimization problems) they are even sufficient (see for example [18, sec. 5.5.3]). For a general optimization problem in the form

$$\begin{aligned} \text{minimize} \quad & f(\mathbf{x}) \\ \text{subject to} \quad & \mathbf{g}(\mathbf{x}) \le \mathbf{0} \\ & \mathbf{h}(\mathbf{x}) = \mathbf{0} \end{aligned} \tag{3.4}$$

with the objective function $f : \mathbb{R}^n \to \mathbb{R}$ and constraint functions $\mathbf{g} : \mathbb{R}^n \to \mathbb{R}^m$ and $\mathbf{h} : \mathbb{R}^n \to \mathbb{R}^p$ the conditions can be expressed as follows.

$$\begin{aligned} \nabla f(\mathbf{x}) + \sum_{i=1}^{m} \mu_i \nabla g_i(\mathbf{x}) + \sum_{i=1}^{p} \lambda_i \nabla h_i(\mathbf{x}) &= \mathbf{0} && \text{Stationarity} \\ \mathbf{g}(\mathbf{x}) &\le \mathbf{0} && \text{Primal feasibility} \\ \mathbf{h}(\mathbf{x}) &= \mathbf{0} && \\ \mu &\ge \mathbf{0} && \text{Dual feasibility} \\ \forall i \in \{1, \dots, m\} \quad \mu_i g_i(\mathbf{x}) &= 0 && \text{Complementary slackness} \end{aligned} \tag{3.5}$$

3.3 Unconstrained QP

In this section, methods for solving unconstrained quadratic programs are discussed and in the end an illustrative example is given.

Since the objective function is strictly convex (we repeat the assumption on $\mathbf{G}$ to be positive definite) and the feasible set $\mathbb{R}^n$ is convex, there is a unique global minimizer. We are looking for a vector $\mathbf{x}^\star$ from $\mathbb{R}^n$ that minimizes the objective function. We can write this as an optimization problem

$$\text{minimize} \quad \frac{1}{2}\mathbf{x}^{\mathrm{T}}\mathbf{G}\mathbf{x} + \mathbf{f}^{\mathrm{T}}\mathbf{x}. \tag{3.6}$$

There is an analytical way to find the solution via KKT conditions (3.5). For this particular case, the conditions reduce to a single stationarity condition. Gradient ∇q of the objective function from (3.2) must equal zero vector. This is actually a linear system of equations:

$$\nabla q = \mathbf{G}\mathbf{x} + \mathbf{f} = \mathbf{0}, \quad \text{and therefore} \quad \mathbf{x}^\star = -\mathbf{G}^{-1}\mathbf{f}. \tag{3.7}$$

Note that the inverse of Hessian matrix $\mathbf{G}$ always exists because it has full rank. The computation of the inverse is not very efficient and a more sophisticated approach exists. Since $\mathbf{G}$ is positive definite, its Cholesky factorization $\mathbf{G} = \mathbf{L}\mathbf{L}^{\mathrm{T}}$, where $\mathbf{L}$ is lower triangular, can be calculated. The original system from (3.7) is then rewritten as

$$\mathbf{L}\underbrace{\mathbf{L}^{\mathrm{T}}\mathbf{x}}_{\mathbf{y}} = -\mathbf{f}. \tag{3.8}$$

This system can be solved in two steps. First, forward substitution in $\mathbf{L}\mathbf{y} = -\mathbf{f}$ yields auxiliary vector $\mathbf{y}$ and then, $\mathbf{x}$ is obtained by backward substitution in $\mathbf{L}^{\mathrm{T}}\mathbf{x} = \mathbf{y}$.

However, it is always not suitable to use this approach. Computation of the inverse or Cholesky factorization may be undesirable. For this reason, several numerical iterative methods exist. Three of them are presented below but many others are stated in the literature (e.g. in [18])

3.3.1 Gradient descent methods

These methods move in the negative gradient direction with the step length t_k. The formula for them is as follows:

$$\mathbf{x}_{k+1} = \mathbf{x}_k - t_k \cdot \nabla q(\mathbf{x}_k). \tag{3.9}$$

The question is, however, how to choose the step length t_k for the method to converge towards the optimum in a fast manner. The criteria for this could be for example Wolfe conditions, see [17, sec. 3.1]. We discuss two options bellow. Other ways are further described in [18, sec. 9.3] or [19].

Fixed step length

The first way of choosing the step length is to set t_k equal to a positive constant t. It is straightforward to implement but the convergence rate may be quite slow.

In order to inspect the convergence of the method, we can use systems theory. Iterative scheme in (3.9) can be viewed as a discrete time dynamic system. It is more evident when we substitute the gradient from (3.2):

$$\mathbf{x}_{k+1} = \mathbf{x}_k - t \cdot (\mathbf{G}\mathbf{x}_k + \mathbf{f}^{\mathrm{T}}) = (\mathbf{I} - t\mathbf{G})\mathbf{x}_k + \mathbf{f}^{\mathrm{T}}. \tag{3.10}$$

For this system to be stable, i.e. to converge to a final value $\mathbf{x}^{\star}$, the poles of the system, the eigenvalues of system matrix $\mathbf{I} - t\mathbf{G}$, must be less than one. This puts a requirement on the step length t because $\mathbf{G}$ is fixed. Once the condition is satisfied, the method asymptotically converges to the optimum.

Exact line search

The other option is to set the step length t_k, such that the step always minimizes q along the ray in the direction of negative gradient. This method finds a point on the ray, at which the objective function is the lowest. The next step then leads to this point.

Thus, the appropriate step length $t_k^{\star}$ has to be found such that (see [18])

$$t_k^{\star} = \arg\min_{t_k \geq 0} q(\mathbf{x}_k + t_k \cdot \Delta\mathbf{x}_k). \tag{3.11}$$

The derivative of q on the ray in the direction $\Delta\mathbf{x}_k$ is expressed and set equal to zero.

$$0 = q'(\mathbf{x}_k + t \cdot \Delta\mathbf{x}_k) \cdot \Delta\mathbf{x}_k = ((\mathbf{x}_k + t \cdot \Delta\mathbf{x}_k)^{\mathrm{T}}\mathbf{G} + \mathbf{f}^{\mathrm{T}}) \cdot \Delta\mathbf{x}_k \tag{3.12}$$

After multiplication and simple manipulation we obtain

$$t_k^{\star} = \frac{-\mathbf{f}^{\mathrm{T}}\Delta\mathbf{x}_k - \mathbf{x}_k^{\mathrm{T}}\mathbf{G}\Delta\mathbf{x}_k}{\Delta\mathbf{x}_k^{\mathrm{T}}\mathbf{G}\Delta\mathbf{x}_k}. \tag{3.13}$$

Because q is a convex function and the ray is a convex set, we conclude that the $t_k^{\star}$ is the minimizer. Thus iterative formula is obtained as

$$\mathbf{x}_{k+1} = \mathbf{x}_k + t_k^{\star} \cdot \Delta\mathbf{x}_k. \tag{3.14}$$

3.3.2 Newton's method

In general, Newton's method solves homogeneous system of equations

$$\mathbf{g}(\mathbf{x}) = \mathbf{0}. \tag{3.15}$$

It starts at some initial guess of the solution and then improves it iteratively.

Instead of solving for the mapping $\mathbf{g}$ it rather substitutes it with its Taylor polynomial of degree one.

$$\mathbf{g}(\mathbf{x}) \approx \mathbf{g}(\mathbf{x_k}) + \mathbf{g}'(\mathbf{x_k})(\mathbf{x} - \mathbf{x_k}) \tag{3.16}$$

Newton's method then solves the system with this modified left hand side. If the Jacobian matrix $\mathbf{g}'(\mathbf{x_k})$ has full rank, the approximated solution can be written in the form

$$\mathbf{x} \approx \mathbf{x_k} - \mathbf{g}'(\mathbf{x_k})^{-1}\mathbf{g}(\mathbf{x_k}). \tag{3.17}$$

The same approach can be used to solve QP. First order optimality condition requires all partial derivatives of the objective q to be zero. That is $\nabla q(\mathbf{x}) = \mathbf{0}$. Obviously, this is a homogeneous system of equations and Newton's method can be used. Plugging into equation (3.17), iterative formula is obtained.

$$\mathbf{x_{k+1}} = \mathbf{x_k} - q''(\mathbf{x_k})^{-1}\nabla q(\mathbf{x_k}) \tag{3.18}$$

Substituting gradient and Hessian matrix of q from (3.2) gives us the result. Note that when $\mathbf{G}$ is positive definite, it has full rank and so the inverse exists. Resulting $\mathbf{x}_{k+1}$ corresponds to analytical solution $\mathbf{x}^\star$ from Equation (3.7).

Detailed derivation can be found e.g. in the book [18].

3.3.3 Example

Methods described above are now presented with a simple two dimensional example. Consider a convex unconstrained QP with objective function $q(\mathbf{x}) = \frac{1}{2}\mathbf{x}^{\mathrm{T}}\mathbf{G}\mathbf{x} + \mathbf{f}^{\mathrm{T}}\mathbf{x}$, where

$$\mathbf{G} = \begin{bmatrix} 2.5 & -7 \\ -7 & 30 \end{bmatrix}, \quad \mathbf{f} = \begin{bmatrix} 2 \\ 4 \end{bmatrix}, \tag{3.19}$$

and starting point is $\mathbf{x}_0 = [4, 2]^{\mathrm{T}}$. Level sets are plotted in the left part of Figure 3.1.

In the red coloring, iterates of fixed step gradient method with step length $t = 0.3$ are shown. The progress of exact line search gradient method is depicted in blue coloring. So called *zig-zag*ing is present. The only step of Newton's method from the starting point $\mathbf{x}_0$ to the optimum is illustrated in green coloring. It corresponds to the analytical solution from (3.7).

Also note the distance to optimum in the right part of Figure 3.1. It is obvious that in this case, fixed step gradient method converges in a slower manner than the one with exact line search. Newton's method gets right to the optimum after the first iterate.

3.4 Equality constrained QP

Equality constrained quadratic program can be written as follows:

$$\begin{aligned} &\text{minimize} && \frac{1}{2}\mathbf{x}^{\mathrm{T}}\mathbf{G}\mathbf{x} + \mathbf{f}^{\mathrm{T}}\mathbf{x} \\ &\text{subject to} && \mathbf{A}_e\mathbf{x} = \mathbf{b}_e, \end{aligned} \tag{3.20}$$

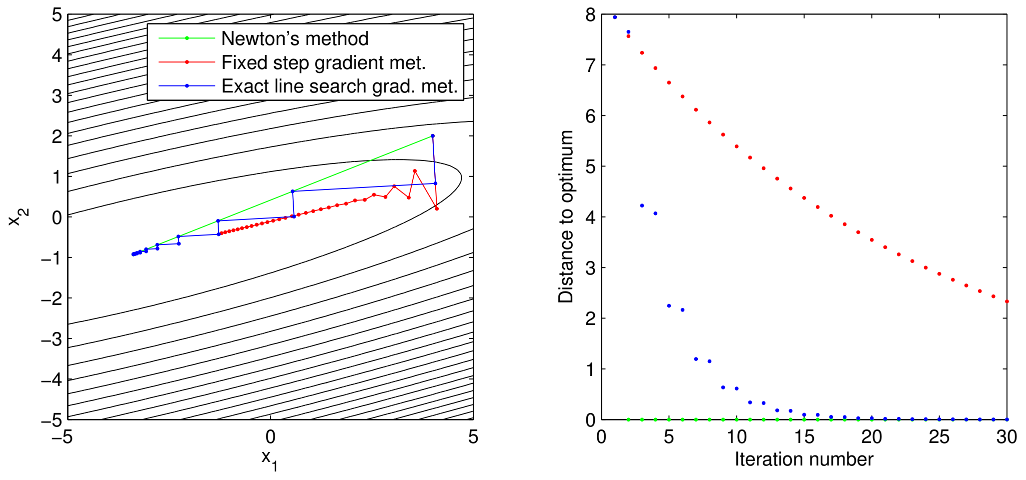

Figure 3.1: The three methods of solving unconstrained QP.

where $\mathbf{A}_e \in \mathbb{R}^{l \times n}$, $l \leq n$ is assumed to have full rank, i.e. the constraints are consistent and they are not redundant. If $\mathbf{A}_e$ was rank deficient, one could remove linearly dependent rows without changing the feasible set.

Such problems are not so frequent in predictive control area. In spite of the fact, they are an important part of optimization methods for inequality constrained QPs. The active set method which we will discuss in the next section, runs an equality constrained minimization algorithm in each iteration.

3.4.1 KKT conditions

KKT optimality conditions for problem (3.20) become well known Lagrange conditions. These are necessary and for convex objective function q with affine constraints they are also sufficient [18]. We can express them in a form

$$\mathbf{G}\mathbf{x}^\star + \mathbf{f} + \mathbf{A}_e^{\mathrm{T}} \cdot \lambda = \mathbf{0}, \quad \mathbf{A}_e \mathbf{x}^\star = \mathbf{b}_e. \tag{3.21}$$

It is possible to rewrite these conditions using block matrix as a system of equations, the KKT system.

$$\begin{bmatrix} \mathbf{G} & \mathbf{A}_e^{\mathrm{T}} \\ \mathbf{A}_e & \mathbf{0} \end{bmatrix} \begin{bmatrix} \mathbf{x}^\star \\ \lambda \end{bmatrix} = \begin{bmatrix} -\mathbf{f} \\ \mathbf{b}_e \end{bmatrix} \tag{3.22}$$

Since $\mathbf{G}$ is positive definite and by assumption $\mathbf{A}_e$ has full rank, the KKT system has unique solution provided that the feasible set is non-empty [18].

Solution of this system leads to the optimal $\mathbf{x}^\star$ and also to the Lagrange multipliers vector λ. Different methods for solving KKT systems are treated in [17, chap. 16]. These methods spread from the direct solution through factorizations to iterative methods.

3.5 Inequality constrained QP

In this section we describe three basic algorithms that solve inequality constrained quadratic programs. Inequality constrained QP can be written in the form

$$\begin{aligned} &\text{minimize} && \frac{1}{2}\mathbf{x}^{\mathrm{T}}\mathbf{G}\mathbf{x} + \mathbf{f}^{\mathrm{T}}\mathbf{x} \\ &\text{subject to} && \mathbf{A}\mathbf{x} \leq \mathbf{b}. \end{aligned} \tag{3.23}$$

Feasible set is described using the inequality $\{\mathbf{x} \in \mathbb{R}^n | \mathbf{A}\mathbf{x} \leq \mathbf{b}\}$. Each row $\mathbf{a}_i^{\mathrm{T}}$ of matrix $\mathbf{A}$ together with corresponding element b_i of vector $\mathbf{b}$ define a half-space $\mathbf{a}_i^{\mathrm{T}}\mathbf{x} \leq b_i$ for $i \in \{1, \dots m\}$. The intersection of these half-spaces is a polytope.

This class of quadratic program is the most general of all (excluding (3.3)) because it can describe equality constrained (using a property $a = b$ if and only if $(a \geq b) \wedge (a \leq b)$) and unconstrained QPs as well.

3.5.1 Active set method

This method makes use of the fact that optimum is often attained on the boundary of the feasible set. In other words, some constraints are usually *active* in the optimum. It means that equality holds for the corresponding row of $\mathbf{A}\mathbf{x} \leq \mathbf{b}$. The set of these constraints is called the *active set* and is denoted $\mathcal{A}$.

Active set method iteratively changes the set of constraints which are active, so called *working set* $\mathcal{W}$. In each step it decides whether to add or remove a constraint from the working set in order to decrease the objective function. This method is closely treated in [17]. Active set approach is quite familiar to those who know the simplex algorithm for linear programming.

The algorithm has to be started with a feasible initial point $\mathbf{x}_0$. Such $\mathbf{x}_0$ is either known in advance or a feasibility linear program known as *phase 1* has to be solved.

Active set method is summarized in Algorithm 3.1 and a brief description follows.

Computation of a step

For each step k, all the constraints that are members of current working set $\mathcal{W}_k$ are treated as equality constraints. The constraints outside $\mathcal{W}_k$ are omitted. Then, an equality constrained quadratic program in the form (3.20) is solved, which provides us with a direction $\mathbf{p}_k = \mathbf{x}^\star - \mathbf{x}_k$ to its optimum.

Once $\mathbf{p}_k = \mathbf{0}$, the optimum with current working set is achieved and the objective cannot be decreased anymore. Thus, Lagrange multipliers λ_i of the equality constrained QP are checked. If all of them are nonnegative, $\mathbf{x}_k$ is the optimizer. Otherwise, one of the constraints with negative λ_i is dropped from $\mathcal{W}_{k+1}$ and a new quadratic program (3.20) with the new set of constraints is solved in order to get a new step $\mathbf{p}_{k+1}$.

If $\mathbf{p}_k$ is nonzero, a step length has to be calculated.

Step length

Maximum step length $\alpha_k \in \langle 0, 1\rangle$ is computed, such that $\mathbf{x_k} + \alpha_k \mathbf{p}_k$ remains feasible. That is, until it reaches any constraint that has been inactive yet (not in the working set). This can be expressed as

$$\alpha_k = \min\left(1, \min_{i \notin \mathcal{W}_k} \frac{b_i - \mathbf{a}_i^{\mathrm{T}} \mathbf{x}_k}{\mathbf{a}_i^{\mathrm{T}} \mathbf{p}_k}\right). \tag{3.24}$$

If no previously inactive constraint is encountered, α_k is set to one. Otherwise, it is set such that it gets to the first (the inner minimum) blocking constraint. The blocking constraint is added to $\mathcal{W}_{k+1}$.

Algorithm 3.1 Active set method for convex QP, [17].

```
Require: Feasible starting $\mathbf{x}_0$, working set $\mathcal{W}_0$.
  for $k = 0, \dots$ do
      Compute step $\mathbf{p}_k = \mathbf{x}^\star - \mathbf{x}_k$ (Equality constrained QP)
      if $\mathbf{p}_k = \mathbf{0}$ then
          Check Lagrange multipliers $\lambda_i$
          if all $\lambda_i \geq 0$ then
              return $\mathbf{x}_k$
          else
              Remove one of $\lambda_i < 0$ from $\mathcal{W}_{k+1}$
              $\mathbf{x}_{k+1} \leftarrow \mathbf{x}_k$
          end if
      else
          Compute $\alpha_k$ from (3.24)
          $\mathbf{x}_{k+1} \leftarrow \mathbf{x}_k + \alpha_k \mathbf{p}_k$
          if blocking constraint found then
              Add it to $\mathcal{W}_{k+1}$
          else
              $\mathcal{W}_{k+1} \leftarrow \mathcal{W}_k$
          end if
      end if
  end for
```

A weakness of this method is its ability to only add or remove one constraint at a time. When the method is started from a point with a few active constraints and there are many constraints active in optimum, a large number of iterations is needed to reach the optimum.

The iterations involve the solution of equality constrained QP, which is equivalent to the solution of KKT system (3.22). This computation is quite costly, but the number of iterates is usually modest and depends on the number of active constraints in the optimum.

Example

In Figure 3.2, a simple two dimensional inequality constrained QP is illustrated. Green lines represent the boundary of the feasible set. The three steps of the active set method are shown in red coloring.

Initial point is $\mathbf{x}_0 = [0, 0]^{\mathrm{T}}$ and working set is $\mathcal{W}_0 = \{1\}$. In the first step, equality

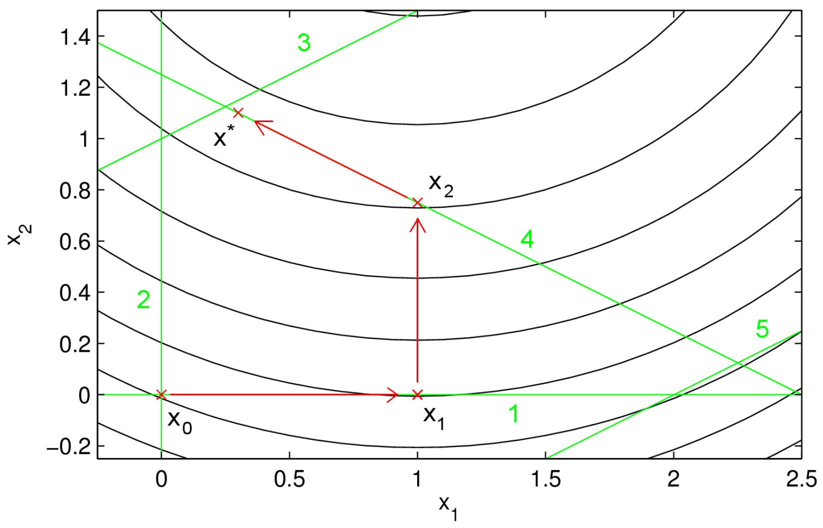

Figure 3.2: Illustration of the active set method for a simple two dimensional problem.

constrained QP (with constraints in $\mathcal{W}_0$) is solved, which provides us a direction to $\mathbf{x}_1$. In the second step, constraint number 1 is dropped from the working set, so $\mathcal{W}_1 = \emptyset$. Then, unconstrained QP is solved, which gives us a direction to the minimum. However, blocking constraint number 4 is encountered and so it is added to the working set $\mathcal{W}_2 = \{4\}$ and a step is taken to $\mathbf{x}_2$ only. Then, equality constrained QP is solved and the optimum $\mathbf{x}^\star$ is found because the objective can no longer be decreased.

3.5.2 Fast gradient method

Fast gradient method was first introduced by Y. Nesterov in 1983 and is also described in [19]. The application of this method to MPC was reported in [7].

It is quite similar to the gradient method for unconstrained optimization. The gradient method itself cannot ensure feasibility of the solution and so a modification has to be made. The negative gradient direction $\nabla q(\mathbf{x}_i)$ in the iterative scheme (3.9) is replaced by the projection of it onto the feasible set.

Gradient projection

However, the projection of this direction onto a general set $\mathcal{Q}$ is a solution $\mathbf{z}^\star$ to an optimization problem

$$\begin{aligned} &\text{minimize} && ||\nabla q(\mathbf{x}_i) - \mathbf{z}||_2 \\ &\text{subject to} && \mathbf{z} \in \mathcal{Q}, \end{aligned} \tag{3.25}$$

which may be equally difficult as the original constrained QP. Thus, this method is only suitable for the constraints, where the projection can be computed easily. These sets include positive orthant, box, simplex or Euclidean norm ball [19]. In the scope of MPC, box constraints are the most significant.

The projection of a vector $\mathbf{a}$ onto a box constrained set in the form $\mathcal{Q} = \{\mathbf{x} \in \mathbb{R}^n | \underline{\mathbf{x}} \leq$

$\mathbf{x} \leq \overline{\mathbf{x}}\}$ can be computed as follows:

$$p(\mathbf{a}) = \operatorname{med}(\underline{\mathbf{x}}, \mathbf{a}, \overline{\mathbf{x}}), \tag{3.26}$$

where the med mapping returns element-wise median of the vector triple.

We can describe the iterative scheme of fast gradient method by Algorithm 3.2. First, a feasible starting point $\mathbf{x}_0$ and an auxiliary vector $\mathbf{y}_0 = \mathbf{x}_0$ is selected. Then, constant step length α_0 is set such that $0 < \sqrt{\frac{\mu}{L}} \leq \alpha_0 < 1$. Numbers L and μ are Lipschitz constant of the gradient and convexity parameter respectively. Both are computed from the eigenvalues of the Hessian matrix. L is the maximal eigenvalue and μ is the minimal eigenvalue [7].

Algorithm 3.2 Fast gradient method for convex QP, [7].

```
Require: Feasible starting $\mathbf{x}_0$
  $\mathbf{y}_0 \leftarrow \mathbf{x}_0$
  $i \leftarrow 0$
  while Stopping condition not satisfied do
      $\mathbf{x}_{i+1} \leftarrow p(\mathbf{y}_i)$                                ▷ using (3.25)
      Solve $\alpha_{i+1}^2 = (1-\alpha_i)\alpha_i^2 + \alpha_{i+1}\frac{\mu}{L}$ for $\alpha_{i+1}$
      $\beta_i \leftarrow (\alpha_i(1-\alpha_i))/(\alpha_i^2 + \alpha_{i+1})$
      $\mathbf{y}_{i+1} \leftarrow \mathbf{x}_{i+1} + \beta_i(\mathbf{x}_{i+1} - \mathbf{x}_i)$
      $i \leftarrow i + 1$
  end while
```

At each step, the point $\mathbf{x}_i$ should be checked for the KKT optimality conditions (3.5). However, this check can take quite a long time, so it is sometimes done only at each k-th step.

Here we repeat that this method is suitable only for the problems where the projection p (3.25) is computed easily. Otherwise, the computation of the projection would break its performance.

The difficulty of individual iterations is mainly caused by the computation of projection (3.25). For a box constrained quadratic program, the computation of projection is quite easy. Aside from the projection, the iterations are quite straightforward.

Compared to the active set method, the active set can change rapidly from iteration to iteration, which decreases the number of iteration needed [17]. However, for ill conditioned problems, the required number of iterates is very large.

3.5.3 Interior point method - Logarithmic barrier

In this subsection we describe one of *interior point* methods, so called *barrier* method. It is dealt in detail in [18]. An application of slightly modified barrier method to model based predictive control is reported in [8].

This method replaces original inequality constrained minimization problem (3.23) with the unconstrained one with modified objective function. Constraints satisfaction is assured by including a barrier function in the objective. The name of the method comes from the fact that the iterates are alway in the *strict interior* of the feasible area.

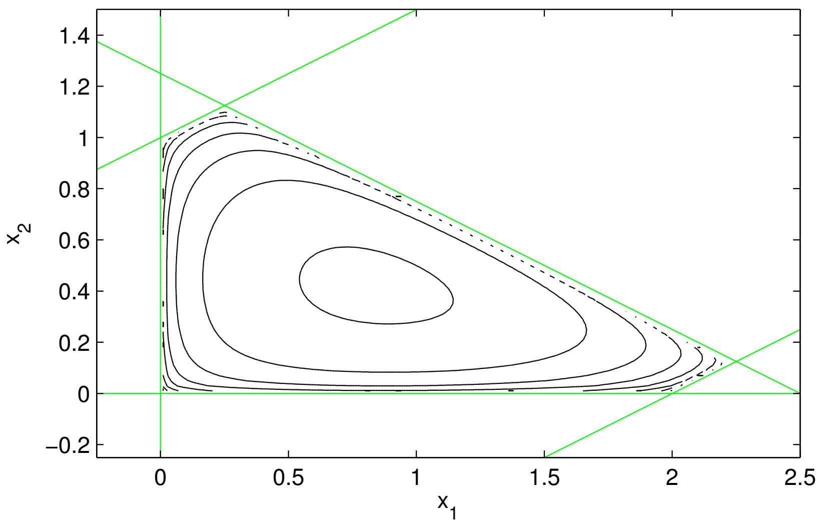

Figure 3.3: Level lines of the barrier function for a sample two dimensional set.

The new unconstrained problem is solved using e.g. Newton's method. Obviously, the solution of the new problem is only an approximation to the original one, because of the influence of the barrier function.

Barrier function

The barrier function value says how close a point $\mathbf{x}$ is to the boundary of the feasible set. We denote the function ψ and define it as follows.

$$\psi(\mathbf{x}) = \sum_{i=1}^{m} -\log(b_i - \mathbf{a}_i^{\mathrm{T}}\mathbf{x}) \quad \text{for} \quad \mathbf{x} \in \mathbb{R}^n \quad \text{satisfying} \quad \mathbf{A}\mathbf{x} < \mathbf{b}. \tag{3.27}$$

Note that the function grows without bound as $\mathbf{x}$ reaches the boundary. This makes the points outside the feasible set unreachable. The ψ is undefined outside the feasible area and on the boundary so a strictly feasible starting point is always required.

Level lines of ψ for a sample two dimensional set are plotted in Figure 3.3.

Modified minimization problem is then expressed as

$$\text{minimize} \quad \frac{1}{2}\mathbf{x}^{\mathrm{T}}\mathbf{G}\mathbf{x} + \mathbf{f}^{\mathrm{T}}\mathbf{x} + \kappa\psi(\mathbf{x}), \tag{3.28}$$

where $\kappa > 0$ determines the quality of approximation of function q by $q + \kappa\psi$ in the feasible region. As κ decreases to zero, ψ influences the objective less and less. Hence, the solution of problem (3.28) gets closer to the solution of the original constrained problem in (3.23).

Sequential decreasing of κ

On one hand, we want number κ to be as small as possible because of the accuracy of solution, but on the other hand, we want it not to be so small because then it would be difficult to solve the unconstrained problem. The latter is due to the rapid change of Hessian near the boundary of the feasible set.

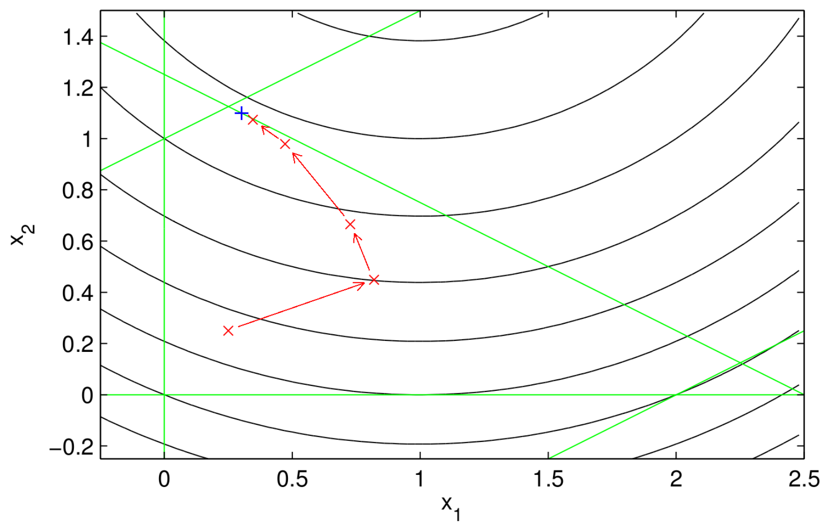

Figure 3.4: Sequence of approximate minimizers of (3.28) for decreasing κ.

To overcome this, the minimization is started with some κ. A few iterations of Newton's method are done (there is no need for the exact minimizer so an approximate solution suffices). After that, κ is decreased by a factor $\nu > 1$ and from the previous solution, new minimization is started.

Parameter ν determines how the objective function in (3.28) differ. If ν is close to one, the individual problems (3.28) are very similar and so less Newton's iterations are required. However, it takes more changes in μ to obtain the same solution. It is a trade-off and values of 10 to 100 usually work well [18].

We can express the idea by Algorithm 3.3.

Algorithm 3.3 Barrier method for convex QP, [18].

```
Require: Strictly feasible starting $\mathbf{x}$, $\kappa > 0$, $\nu$
  while Stopping condition is not satisfied do
      Minimize $q + \kappa\psi$ starting from $\mathbf{x}$          ▷ using e.g. Newton's method
      $\kappa \leftarrow \kappa/\nu$
      $\mathbf{x} \leftarrow \mathbf{x}^\star$
  end while
```

The iterates of interior point method are quite costly because they involve Newton's method. Hence, linear system has to be solved at each step. However, the number of iterations required to reach the optimum is relatively modest.

Example

In Figure 3.4 a sequence of approximate minimizers $\mathbf{x}^\star$ of (3.28) for different values of κ is shown. The minimization was started with $\kappa = 10$ and it was decreased by the factor $\nu = 10$ at each step. It can be clearly seen that as κ decreases, the minimizer of $q + \kappa\psi$ gets closer to the one of the original constrained quadratic program (the blue cross).

Chapter 4

Properties of QP algorithms

In this chapter the properties of selected QP algorithms will be shown. We especially treat the computation time of the algorithms, because it is crucial to the ability to control fast dynamic processes. Several factors that influence the computation time will be studied via numerical simulations. We will only study strictly convex quadratic programming algorithms with bound constraints. The number of optimization variables will be sometimes referred to as *QP size* throughout the chapter.

The chapter is organized in the following manner. The first section presents the solvers making use of inequality constrained QP algorithms from Section 3.5. In the second section, numerical experiments are carried out and the results are discussed. The section is divided into two subsections. The first of them shows model predictive control example and the second one randomly generated quadratic programs. The third section summarizes the results of the experiments.

4.1 QP solvers under test

In this section we briefly present the solvers to be tested in this chapter. Representatives of each algorithm from the previous chapter were selected. General purpose solvers (quadprog, MOSEK) as well as those specific to MPC (qpOASES and FiOrdOs) are described.

4.1.1 quadprog - Active set method

As a part of the Optimization toolbox in Matlab, quadprog represents an ordinary active set algorithm. It does not have any option to utilize the sequential nature of the QPs arising in model based predictive control and it is not intended to be used in fast applications. For more information, please see Matlab help (`http://www.mathworks.com/help/optim/ug/quadprog.html`).

4.1.2 qpOASES - Specialized active set method

This solver was specifically designed to fit MPC. It uses so called extended online active set strategy. It makes use of the fact that the QPs arising in MPC differ in vector $\mathbf{f}$ which is a function of system state. The state space can be partitioned into critical regions much like in explicit MPC [13]. On the path from the previous state to the current one, the knowledge about the regions is used to identify the optimal active set faster. It is similar to warm starting. For further details see [6].

The program is written in C++ with an interface to Matlab. The latest version available (3.0 beta) was used (minor stability issues were encountered). The source code and the installation instructions are published on-line at `http://www.kuleuven.be/optec/software/qpOASES`.

4.1.3 FiOrdOs - Fast gradient method

Strictly speaking, FiOrdOs is not a solver but a code generator. It generates a C code to be compiled, and an interface to Matlab. The resulting program solves QPs using fast gradient method (see [7]). FiOrdOs can be downloaded as a Matlab toolbox from `http://fiordos.ethz.ch`. Documentation is available as a part of the toolbox only.

The solver can handle general inequality constraints ($\mathbf{Ax} \leq \mathbf{b}$), but as it calculates the projection on the feasible set (see Equation (3.25) in the previous chapter), it becomes very slow. Therefore, we use only simple bound constraints on variables.

4.1.4 MOSEK - Interior point method

MOSEK is an optimization package to solve linear, quadratic, general non-linear and mixed integer optimization problems. Interfaces to Matlab are included. The QP solver uses interior point algorithm and is well suited for large scale problems. It is a general purpose solver and is not intended for fast MPC applications. We include it to compare MPC specific solvers to the ordinary ones. Documentation can be downloaded on-line at `http://docs.mosek.com/6.0/toolbox.pdf`.

Although the package is commercial, academic license is available for research purposes. For the test, the default options were used.

4.1.5 Fast MPC - Specialized interior point method

This approach originates to [8]. Several modifications to the interior point method (Section 3.5.3) are made in order to decrease the computation time.

Wang and Boyd proposed using a single value of κ and stopping the minimization after a fixed number of Newton iterations. In addition, they made use of banded structure of the Hessian matrix (which allowed fast Newton's step calculation), because they used different (sparse) MPC formulation. These modifications make their approach very fast. The resulting solution is only a rough approximation to the exact optimizer but they shown that the resulting control quality is comparable to the one obtained with exact QP solution.

Unfortunately, their code (available at `http://www.stanford.edu/~boyd/fast_mpc/`) only runs simulations of the regulator problem. It does not allow direct QP solution, so it cannot be used. The speed however is impressive.

We prepared a Matlab substitute `interior_point`, which implements the algorithm from the above mentioned paper without exploiting the Hessian structure. However, its performance is poor compared to the original code or to the other MPC specific solvers.

4.2 Numerical experiments

This section describes two types of numerical experiments. The experiments are chosen to illustrate typical properties of QP algorithms regarding the computation time. The first experiment simulates the run of MPC controller while the second one studies the solution of randomly generated quadratic programs.

All numerical experiments were carried out on a notebook PC with Intel Core 2 Duo 2.1 GHz CPU running 32 bit Ubuntu 10.04 LTS with Linux 2.6.32 kernel. An interface for quadratic program generation and for solver calling was written in Matlab R2011b. The source code is attached to this thesis so that one can experiment with MPC and the solvers.

4.2.1 Computation time measurement

Optimization run-times were measured using `tic` and `toc` functions as recommended by the MathWorks (the producer of Matlab) in [20]. These times do not include the phase 1, i.e. obtaining a feasible starting point. Additionally, Matlab process was being run with highest priority so as to decrease the influence of the remaining processes. All the tests were performed twice and the minimum of the run-times was taken.

4.2.2 Model predictive control example

In order to show the typical features of QP solvers, we will run them in model predictive controller for a MIMO (multiple input multiple output) dynamic system. The system is a laboratory model of a helicopter. State space model was identified in [21]. It has two inputs (main rotor voltage and tail rotor voltage) and two outputs (elevation angle and azimuth angle).

Both inputs are constrained to be within ± 1 V. The outputs are to track desired reference signals with step changes.

The sampling time is 0.01 s. If it was a real world control, the optimization would have to be computed by the end of the sample. However, the example is intended just to show the properties of the solvers, so we do not enforce this time limit anyhow.

Parameters of the controller are $n_p = 100$ and $n_c = 20$. Weighting matrices $\mathbf{Q} = 10\mathbf{I}$ and $\mathbf{R} = \mathbf{I}$. The size (i.e. the number of variables) of resulting QP which has to be solved at each time step is $2 \cdot n_c = 40$.

Output reference tracking as well as computed control actions are shown in Figure 4.1. One can see how the control action hits the limit several times (around 0.2 s, 0.5 s and 1 s) because the reference signal changes rapidly.

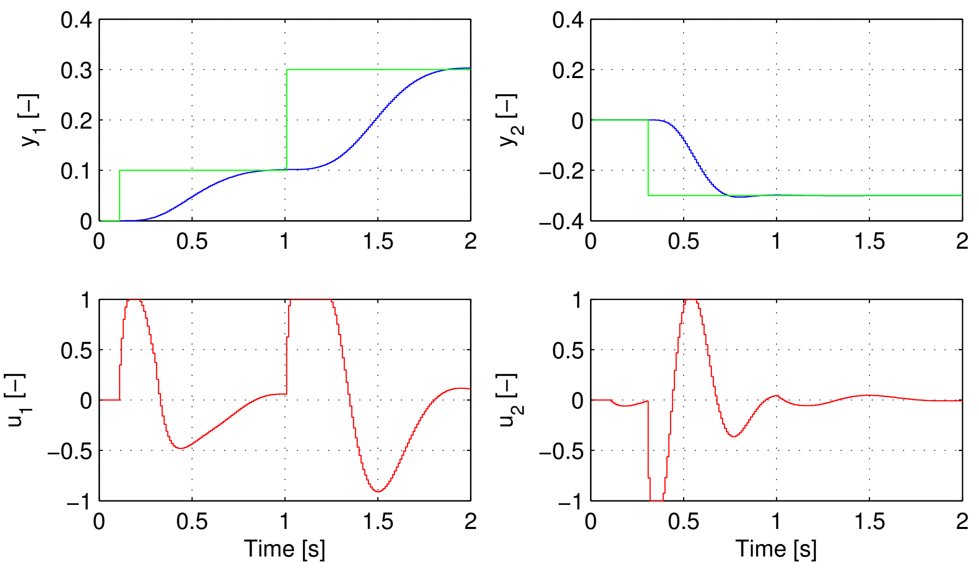

Figure 4.1: Reference tracking MPC (upper part) together with control actions (lower part).

Typical computation time evolution

Here, we present a typical computation time evolution for a series of quadratic programs during MPC simulation for the solvers given above. For the control problem described in Subsection 4.2.2, simulation was performed using all the solvers.

In Figure 4.2, computation times are shown. Not surprisingly, as the reference changes, the active constraints sets differ in time. Hence the computation time of the active set solvers (qpOASES, quadprog) exhibits apparent increase. It can be seen, that unlike quadprog, qpOASES uses specialized warm starting technique. Note that after the increase in computation time, for the next sample it required only very few iterations. This is in contrast with quadprog, which required only slightly less iterations.

FiOrdOs also needed slightly more iterations and thus more time. On the other hand, interior point solvers (MOSEK, `interior_point`) hold the computation time almost constant.

Clearly, specialized solvers such as qpOASES and FiOrdOs outperform the general purpose ones. Both of them could be used to control the system because the computation time easily fits into the sampling time.

Number of variables

To illustrate the computation time dependency on the QP size the following experiment has been done. The same MPC simulation from Subsection 4.2.2 as in the previous part was run. The number of variables $n_c \cdot n_u$ was set using the correction horizon $n_c \in \{5, 10, \dots 100\}$ which makes it vary from 10 to 200.

In Figure 4.3, computation times for the whole MPC simulation and varying problem size are plotted. There are two things to be noted. First, active set solvers (qpOASES and quadprog) share the increase in computation time with the active set change. It is even

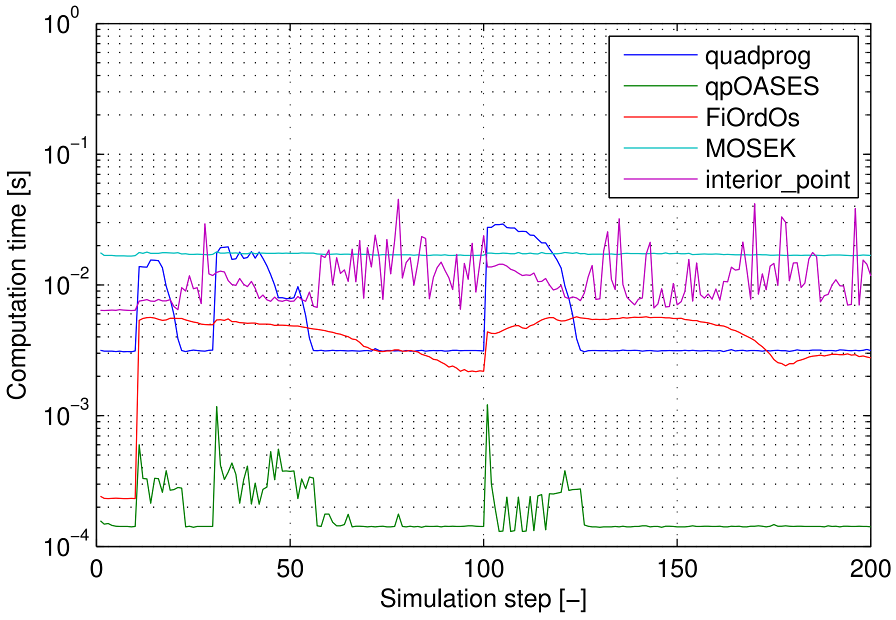

Figure 4.2: Typical computation time evolution for MPC simulation. QP size is 40 (see 4.2.2) for all the solvers.

more obvious with larger QP size. However, qpOASES is far faster because of its modified warm staring feature. After the reference change (step number 100 in Figure **??**), the active set it identified and then, the next step is calculated in much less time.

Second, interior point solvers keep the computation time almost constant over the whole simulation. These are the features of the algorithms that we have already seen in the previous part (in Figure 4.2).

MOSEK performs well with larger QPs (from the point of view of general optimization these are small scale ones) but it is rather slow with smaller ones. This is most likely due to the analysis and modification of the problem that takes place prior to the actual solution (presolve phase). It takes considerable amount of time which can be neglected when the number of variables is in the order of hundreds or thousands, but not tens.

Q and R penalty matrices

In this part we review the influence of $\mathbf{Q}$ and $\mathbf{R}$ matrices on the computation time of the solvers. MPC simulation for the problem from Subsection 4.2.2 was run. Correction horizon was set to $n_c = 20$, weighting matrices to $\mathbf{R} = \mathbf{I}$ and $\mathbf{Q} = \alpha\mathbf{I}$ with varying parameter α.

This setting influences the quality of reference tracking as well as the input activity. The larger is α, the tighter the tracking, but the more aggressive the control.

The effect of large α is illustrated in Figure 4.4. There, solid line shows reference tracking with parameter α set to 10^4. Especially note the control action (lower part of figure) and compare it to the one with $\alpha = 10$ which is depicted in dashed line.

The computation time median over the whole MPC simulation (200 quadratic programs) is plotted against varying α for all the solvers in Figure 4.5a. Obviously, fast

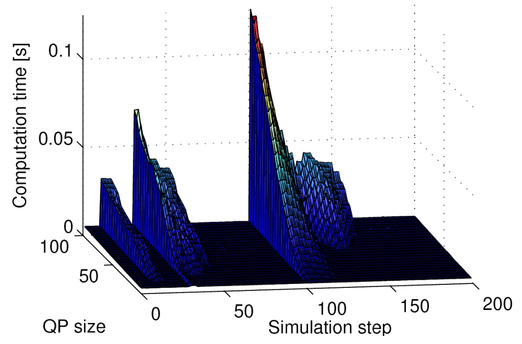

(a) quadprog

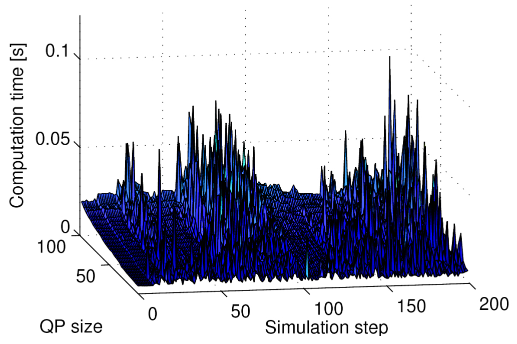

(b) interior point

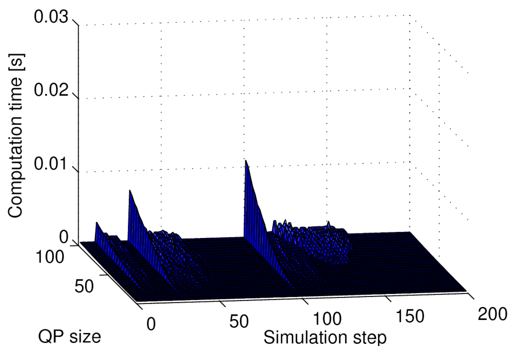

(c) qpOASES

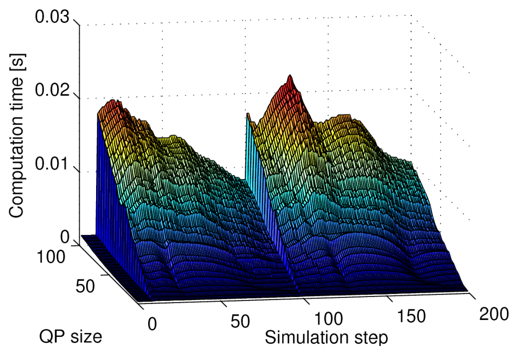

(d) FiOrdOs

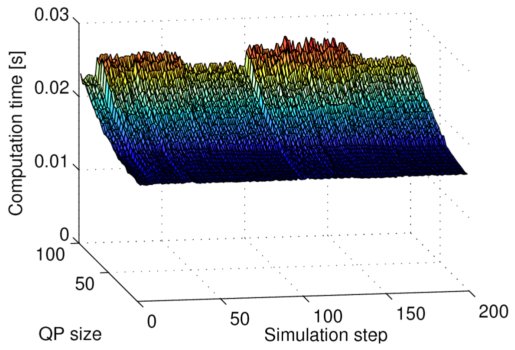

(e) MOSEK

Figure 4.3: Computation time versus QP size.

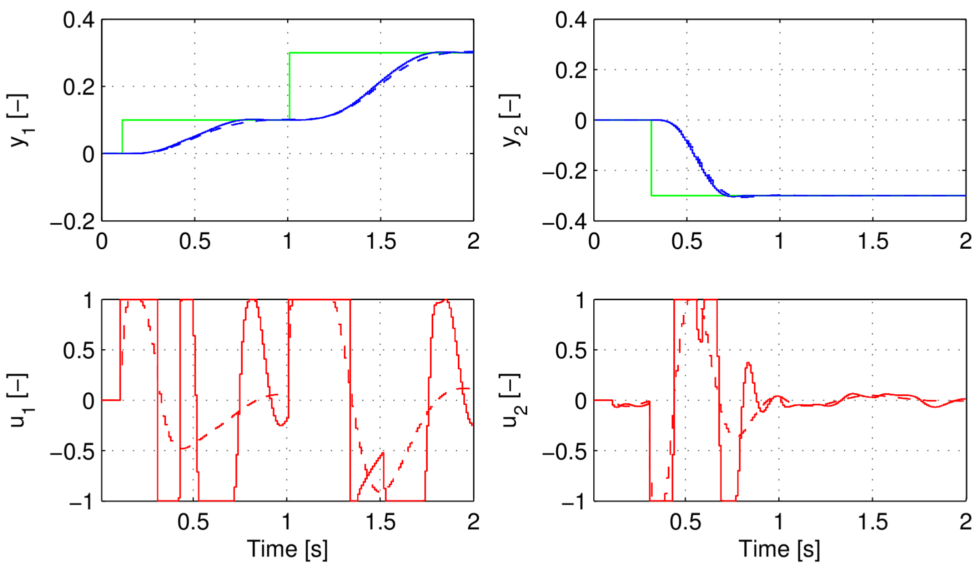

Figure 4.4: Influence of penalty matrix weight on the control quality. Solid line: $\alpha = 10^4$, dashed line: $\alpha = 10$.

gradient method of FiOrdOs performs worse and worse as α increases.

That is because **Q** and **R** matrices also influence *condition number* of QP Hessian matrix. Condition number of a square matrix is a ratio of its largest singular value to the smallest. In Figure 4.5b condition number of **G** is plotted as a function of parameter α.

Evidently, condition number grows with α. In [7] an upper bound on iteration number is given as a function of condition number and required suboptimality. The number of iterations grows with condition number and so does the computation time. It is a typical property of gradient methods.

Active set algorithms also show some increase in the computation time but it is rather due to the more aggressive control that jumps from one limit to the other (see Figure 4.4) and makes the active set change rapidly. Therefore, more iterations are needed to reach the optimum.

Computation times of interior point solvers are almost unaffected by the condition

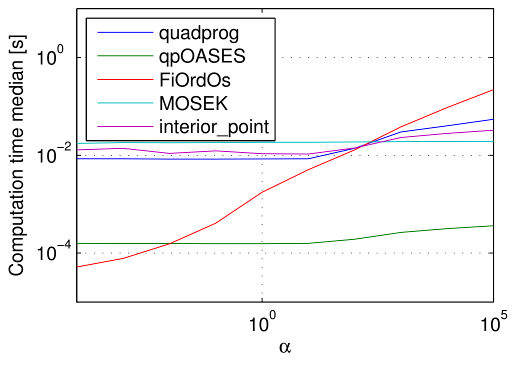

(a) Influence α on the computation time.

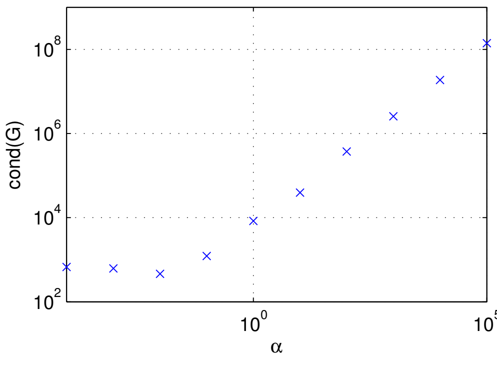

(b) Influence of α on the condition number.

Figure 4.5: Effect of penalty matrix **Q** weight α. Note the computation time of FiOrdOs that is strongly affected by the condition number.

number.

4.2.3 Random QP

In this Subsection, the properties of QP solvers will be presented on the set of randomly generated quadratic programs. The first part presents the generation of random QPs. The second one shows the computation times as a function of the problem size and the number of active constraints in optimum.

We regard ith constraint as active if $\mathbf{a}_i^{\mathrm{T}}\mathbf{x} - b_i + 10^{-7} \geq 0$. Strict equality is not required because of possible numerical errors etc.

We exclude `interior_point` solver from this experiment because even with the tolerance set to 10^{-3}, the number of constraints satisfying the above mentioned condition was different from the one obtained by the rest of solvers. It provides only an approximate solution to quadratic programs. The solution is influenced by the logarithmic barrier which restricts constraints activation. In other words, the method cannot get right on the constraint because there is a nonzero barrier function value (see the level lines of the barrier function in Figure 3.3).

Active set solver qpOASES was used without its warm starting feature because the nature of this experiment does not allow it. There is no meaningful sequence of quadratic programs.

Generation of convex quadratic programs

In order to generate convex quadratic program, we need to get positive semidefinite n by n Hessian matrix $\mathbf{G}$, column vector $\mathbf{f}$ and lower ($\underline{\mathbf{x}}$) and upper ($\overline{\mathbf{x}}$) bounds on variables.

Positive definite Hessian matrix $\mathbf{G}$ is constructed from its singular value decomposition (SVD). For any symmetric positive definite matrix, its SVD equals its eigenvalue decomposition [17, A1].

$$\mathbf{G} = \underbrace{\mathbf{U}\mathbf{S}\mathbf{V}^T}_{\text{SVD}} = \underbrace{\mathbf{A}\mathbf{E}\mathbf{A}^{-1}}_{\text{eigenval. d.}} = \mathbf{A}\mathbf{E}\mathbf{A}^T \tag{4.1}$$

Here, $\mathbf{A}$ is orthogonal ($\mathbf{A}^{-1} = \mathbf{A}^{\mathrm{T}}$) and $\mathbf{E}$ is diagonal and contains eigenvalues (singular values) of $\mathbf{G}$.

Orthogonal $\mathbf{A}$ is generated from a QR decomposition of random matrix with normally distributed elements. $\mathbf{E}$ is generated as a diagonal matrix with positive elements. These elements are the eigenvalues of $\mathbf{G}$ and they determine the condition number and ensure positive definiteness.

Vector $\mathbf{f}$ is generated as a column vector with normally distributed elements with zero mean and unit variance.

Bounds on variables (column vectors from $\mathbb{R}^n$) are generated such that the problem is feasible. That is, the feasible region is non-empty. To do this, we generate random lower bound vector $\underline{\mathbf{x}}$ with normally distributed elements. Then, we get the upper bound $\overline{\mathbf{x}} = \underline{\mathbf{x}} + \mathbf{c}$, where $\mathbf{c}$ is random positive vector with uniformly distributed elements on $(0, k)$.

Parameter k, i.e. the width of a band, was being adjusted so that the number of active constraints spread from 0 to n.

Condition number of Hessian matrix $\mathbf{G}$ was set to be in order of 10^4 to 10^6. Quadratic programs were generated with varying number of variables $n \in (1, \ldots, 100)$. There were $10 \cdot n$ random quadratic programs for each problem size. This resulted in a set of 50500 QPs.

These problems were solved by the four solvers (excluding `interior_point`). Mean computation time was calculated for each QP size and for each number of active constraints.

Results

Mean computation times are plotted against quadratic program size and number of active constraints in the optimum in Figure 4.6.

Overall, quadprog is the slowest. The computation times reach 0.5 s for the larger QP sizes with many active constraints.

Both active set solvers suffer from increasing computation times for growing number of active constraints. The computation times required by qpOASES are much longer than those observed during MPC simulation in Figure 4.3. In this experiment, there is no sequence of quadratic programs and so no warm starting took place.

Fast gradient method even decreases the time needed with the growing number of active constraints. This is caused by the projection onto the feasible set. Once the calculated step points outside the feasible set, it is projected onto it and the corresponding constraints are activated (see projection formula (3.26)).

With a few active constraints, fast gradient method exhibits typical feature of gradient methods: slow convergence rate when the problem is not well conditioned [22]. Its behavior then resembles e.g. the one of gradient method with exact line search seen in Figure 3.1.

Interior point solver MOSEK is unaffected by the number of active constraints in the optimum.

4.3 Summary

In this chapter, properties of inequality constrained quadratic programming algorithms were studied. Five solvers using modified algorithms from Section 3.5 were put under test.

Active set methods Active set algorithms need relatively small number of quite demanding iterations that include the solution of linear KKT system. It is only possible to add or remove one constraint from the active set at a time. Hence, when there are many constraints active in the optimum, many iterations are needed. This was illustrated in Figure 4.6.

Fast gradient method Computation time of fast gradient method strongly depends on the condition number. This was shown in Figure 4.5. With a few active constraints,

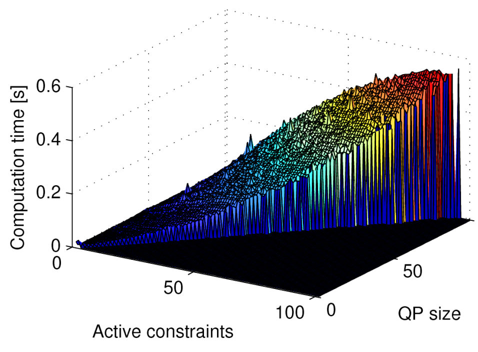

(a) quadprog

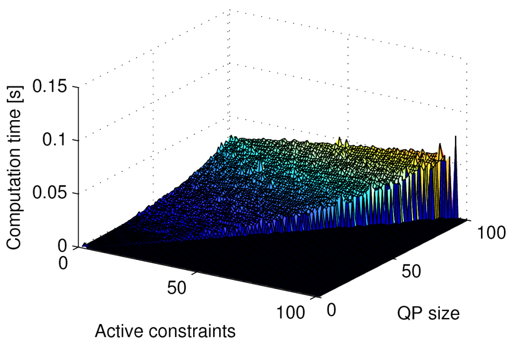

(b) qpOASES

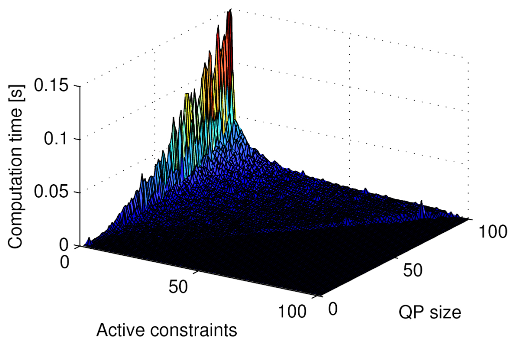

(c) FiOrdOs

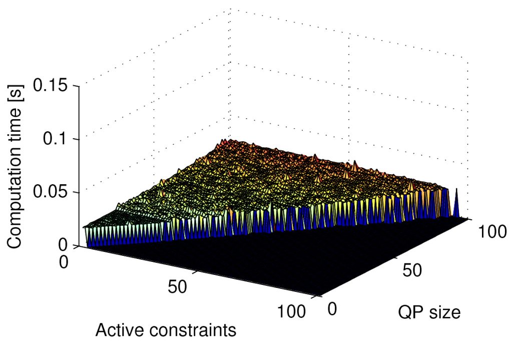

(d) MOSEK

Figure 4.6: Mean computation time as a function of QP size and number of active contraints in optimum for random QPs.

this becomes the most apparent as can be seen in Figure 4.6c.

Interior point methods Computation time of interior point algorithm does not depend on the number of active constraints in optimum. This property was shown in Figure 4.6d. It has almost no dependence on the condition number as was demonstrated in Figure 4.5.

MOSEK is intended for large scale optimization problems and so it analyzes the problem prior to the solution which makes it relatively slow with small scale problems (tens of variables). However, with random QPs and larger scale problems (Figure 4.6d), it was faster than qpOASES (because it had no sequential advantage here) and faster than FiOrdOs for small number of active constraints.

MPC specific vs. general purpose solvers Solvers that are specifically designed for model based predictive control applications, such as qpOASES and FiOrdOS, perform very well during MPC simulations. General purpose solvers such as quadprog or MOSEK are not intended for this use and so they are not as good. However, the later one performed very well. With randomly generated problems it was one of the fastest, except for the small scale problems, where the analysis of the problem slowed it down (see Figure 4.3e).

Chapter 5

Robustness of unconstrained MPC

In this chapter we discuss the robustness of unconstrained model predictive controller. For a detailed survey on robust predictive control analysis and design see e.g. [23]. It is a broad topic to treat so we restrict our scope to the robustness in terms of control performance.

The chapter is organized as follows. First, the influence of uncertain system parameters on the closed-loop reference step response is illustrated. A simple second order open-loop stable system is chosen and its parameters are varied while the predictive controller remains the same.

Then, the effect of control horizon on robust control performance is discussed. Benchmark systems are proposed, and a predictive controller is constructed for each of them. Then, system parameters are varied in the surroundings of the nominal (exact) model and their influence on closed loop response is studied. This is done by means of Monte Carlo simulation.

5.1 Influence of uncertain system parameters

This section illustrates the influence of system-model mismatch caused by incorrect system parameters. We assume that the structure of a model and a system is the same and so the mismatch is caused only by the uncertain parameters. The uncertain parameters may present for example modeling or system identification inaccuracy or the change in the system under operation.

The mismatch between the model and the system results in prediction mismatch. The predicted behavior and the real behavior differ and so the controller makes wrong decision. It leads to poor tracking performance as will be shown below.

In order to avoid this, special measures would have to be taken. The effect of inaccuracy in the model is similar to the effect of constant disturbance [23]. Therefore, disturbance estimation can be used to compensate the inaccurate model. Methods such as *unknown input observer* are quite common. In [24], the authors included a disturbance model into state space description and achieved robust offset-free tracking of various classes of reference signals.

However, we did not make any modification to the MPC that was described in Section 2.4.

5.1.1 Example

As an example, we present a simple second order SISO system. It is a continuous time system and we discretize it using zero-order-hold (`c2d` function in Matlab) with sampling time T_s such that there is approximately 20 samples per rise time. Then, we treat is as a discrete time system and design model predictive controller. The transfer function of this system is as follows:

$$H(s) = \frac{Ke^{-s \cdot d \cdot T_s}}{(0.25s+1)(as+1)}, \tag{5.1}$$

where $T_s = 0.028$ s is sampling time and nominal parameter values are $K_0 = 1$, $a_0 = 0.1$ and $d_0 = 0$. That means open-loop stable system, with zero time delay. Parameter d determines the length of time delay.

Model predictive controller parameters were set to $n_p = 40$, $n_c = 10$, $\mathbf{Q} = \mathbf{I}$ and $\mathbf{R} = \mathbf{I}$. Prediction horizon length is sufficient to include all important dynamics of the open-loop step response.

Now, the parameters will be varied and the effect on the closed loop response will be shown. Closed loop response of nominal system with model predictive controller is always shown in red coloring. In the literature (e.g. in [25]) the influence of system-model mismatch is described in more sophisticated ways. Here, only unit step responses are depicted.

Gain K

In Figure 5.1a, gain K of the system is varied in the range ± 20 % around the nominal value K_0. The grey lines show the response with perturbed parameters. Note that the controller succeeds in offset-free reference tracking only with nominal system. When the actual parameter is less than nominal, i.e. the controller overestimates the response, closed loop response is less than required to achieve the reference signal. On the other hand, when the true parameter is greater than nominal, closed loop response is too high.

Time constant a

Figure 5.1b shows the effect of varying time constant a (a_0 plus minus 20 %). Note that the change in a does not affect DC gain of the system. It seems the same as the effect of gain, but on a closer inspection, a slight difference appears. The responses in Figure 5.1a are only scaled up or down, but here, the shapes slightly differ. It is the most obvious when one compares the largest and the smallest curve. On the largest curve, from sample 20 on, the line is almost straight. On the smallest one, the curve is bent down.

Delay d

The effect of input delay not included in the model is shown in Figure 5.1c. Increasing the delay from 0 to 10 samples causes the closed loop to oscillate. When the delay is grater than 6 samples, the system becomes unstable. This may be caused by the length of prediction horizon. According to [26], the prediction horizon should be increased by the number of delay samples.

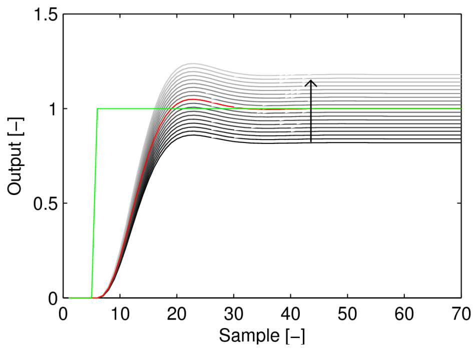

(a) Variation in gain K.

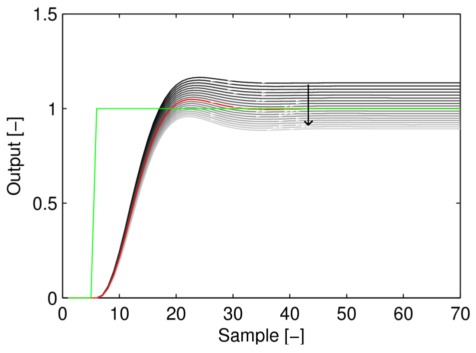

(b) Variation in time constant a.

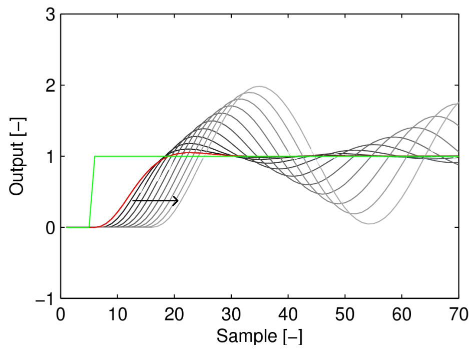

(c) Variation in delay d.

Figure 5.1: Step response of nominal (red) and perturbed (grey) system with varying parameters. The arrows indicate increase in uncertain parameters.

5.2 Influence of control horizon

In this section, the effect of varying control horizon on control performance in presence of system-model mismatch will be studied. First, *mean stage cost*, a measure of the quality of control for a model predictive controller constructed according to Section 2.4 will be shown. Then, closed loop responses to reference unit step are studied and compared in terms of mean stage cost during Monte Carlo simulation.

Stage cost C is a sum of squared tracking errors $\mathbf{e}_i$ and squared control increments $\Delta\mathbf{u}_i$ weighted by $\mathbf{Q}$ and $\mathbf{R}$ matrices as in (2.29). Mean stage cost C_m is a cost per simulation step and it is given by the following formula:

$$C_m = \frac{1}{n_s} C = \frac{1}{n_s}\frac{1}{2}\left(\sum_{i=1}^{n_s} \mathbf{e}_i^{\mathrm{T}}\mathbf{Q}\mathbf{e}_i + \sum_{i=1}^{n_s} \Delta\mathbf{u}_i^{\mathrm{T}}\mathbf{R}\Delta\mathbf{u}_i\right), \tag{5.2}$$

where n_s is the number of simulated steps. The only difference between stage cost C and cost function J in (2.29) is that in the latter one summation happens over predicted errors and future control increments, in this section, we sum real errors and control increments applied to the system during the simulation.

5.2.1 Nominal models and controller tuning

All the systems are second order single input single output (SISO) continuous-time systems with various uncertain parameters. The control objective is to track output reference step signal.

The systems are discretized with zero-order-hold and then treated as discrete time systems. Hence, model based predictive controller can be used. The sampling time is set is set such that it covers the dynamics well.

These systems represent typical simplified models of various processes.

System A: Two real poles + gain

Continuous time transfer function is given as follows:

$$H(s) = \frac{K}{(0.25s+1)(as+1)}, \tag{5.3}$$

where nominal parameter values are $K_0 = 1$ and $a_0 = 0.1$. Sampling time is 0.028 s. Step response of the discretized system is plotted in Figure 5.2a.

System B: Integrator

$$H(s) = \frac{K}{s(as+1)} \tag{5.4}$$

There are two uncertain parameters with nominal values $K_0 = 1$ and $a_0 = 0.25$. Sampling time was set to 0.05 s. Step response of the discretized system is plotted in Figure 5.2b.

System C: Two real poles + unstable zero

This system has an unstable zero. Transfer function is given as follows:

$$H(s) = \frac{K(bs-1)}{(0.25s+1)(as+1)}, \tag{5.5}$$

with nominal parameter values $K_0 = 1$, $a_0 = 0.1$ and $b_0 = 0.5$. Sampling time for this system is 0.014 s. Step response of the discretized system is plotted in Figure 5.2c.

System D: Transport delay

This system includes input transport delay.

$$H(s) = \frac{e^{-s\cdot d\cdot T_s}K}{(0.25s+1)(as+1)}, \tag{5.6}$$

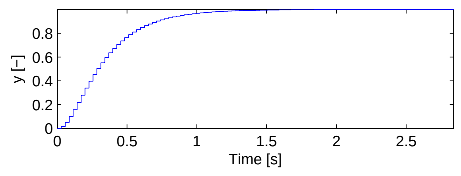

(a) System A

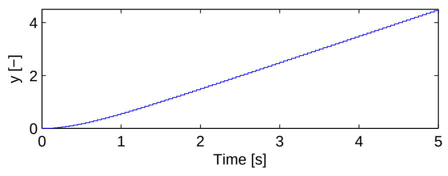

(b) System B

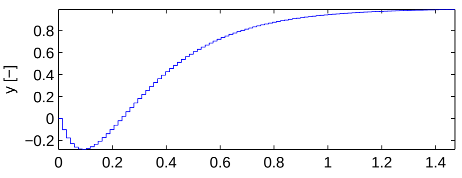

(c) System C

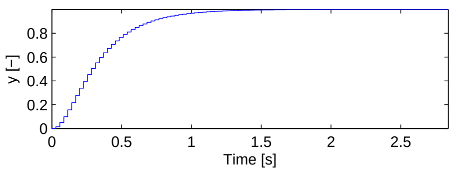

(d) System D

Figure 5.2: Step responses of the nominal models.

with nominal parameters $K_0 = 1$, $a_0 = 0.1$ and $d_0 = 0$. Note that in the nominal model, there is no delay. It is rather put into the system to be controlled, which causes the effect that was shown in Figure 5.1c. Sampling time is the same as the one for system A, that is $T_s = 0.028$ s. Step response of the discretized system is plotted in Figure 5.2d.

Controller tuning

Model predictive controller was set up by trial and error such that it ensured reasonably good reference tracking with the nominal system. Prediction horizon was always set to $n_p = 40$. This is sufficient to include all important dynamics and steady state of the open-loop step response (impulse response in case of system B). Weighting matrices are identity matrices of appropriate size: tracking error penalty $\mathbf{Q} = 100\mathbf{I}$ ($10\mathbf{I}$ for system D) and control increment penalty $\mathbf{R} = \mathbf{I}$.

5.2.2 Monte Carlo simulation

The parameters are set with uniform distribution at the interval ± 20 % around the nominal value. The only exception to this rule is the delay in 5.2.1, which was generated from the set $\{0, 1, 2, 3\}$. All the parameters were changed simultaneously.

The control horizon n_c was successively set to 1, 2, 5 and 10 samples respectively. For each n_c there were 500 simulation runs with all the systems from the previous subsection.

With all the data collected, mean stage cost C_m from (5.2) was evaluated. Then the histograms of mean stage cost were plotted. The results are discussed bellow.

System A

The resulting histogram is shown in Figure 5.3a. Notice a red vertical line that shows mean stage cost for the nominal system. Obviously, as we increase the control horizon from one to two samples, nominal mean stage cost decreases. The decrease at the change from two to five or from five to ten is not that significant. This is a well known behavior and it is described e.g. in [1].

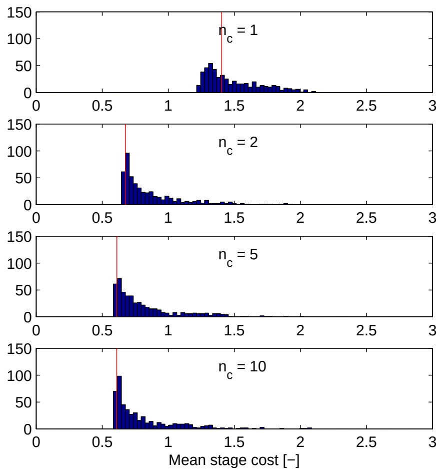

(a) System A

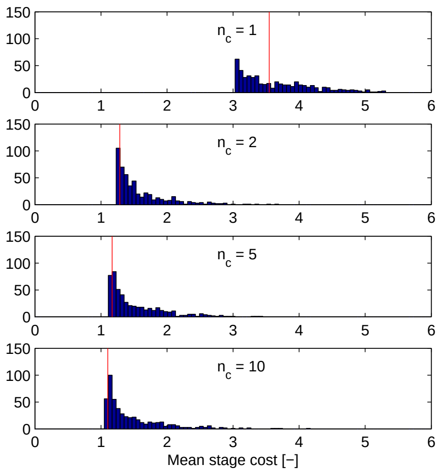

(b) System B

Figure 5.3: Histogram of mean stage cost. Red line shows cost with nominal system.

System B

The results are shown in Figure 5.3b. There is significant decrease in mean stage cost when the control horizon is set to 2 instead of 1.

System C

The results for the system with an unstable zero are plotted in Figure 5.4a. The increase in control quality is much almost insignificant when n_c increases from 1 to 2. It is in contrast with systems A and B. This is true even for the nominal system. This is caused by the fact that the tracking error is dominated by the negative response coming from the unstable zero. The range of costs remains roughly the same for all the control horizon lengths.

System D

For this system, different weighting matrix $\mathbf{Q} = 10\mathbf{I}$ was used. The reason for this is that with $\mathbf{Q} = 100\mathbf{I}$ the system became unstable even with one sample delay.

The results for system D are plotted in Figure 5.4b. Nominal system's cost exhibits similar decrease with growing control horizon. However, for control horizon five and ten the oscillation (illustrated in Figure 5.2d) became more intensive. Hence, the cost exceeded 0.4. This suggests that the controller might be slightly less robust to system-model mismatch when an unmodelled input delay is present and n_c is relatively large.

Summary

The effect of increased control horizon on the control quality is quite apparent for all the systems except the one with unstable zero. This is probably due to the negative response coming from the transfer function zero. Control horizon set to one gave the

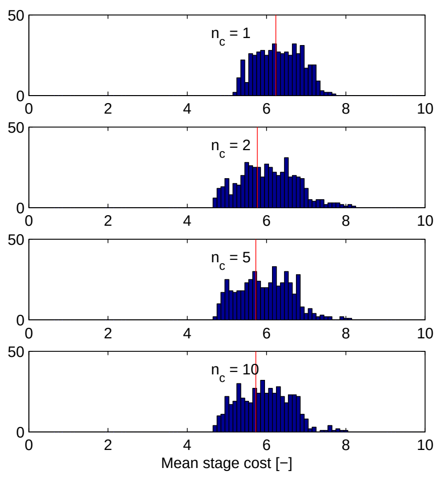

(a) System C

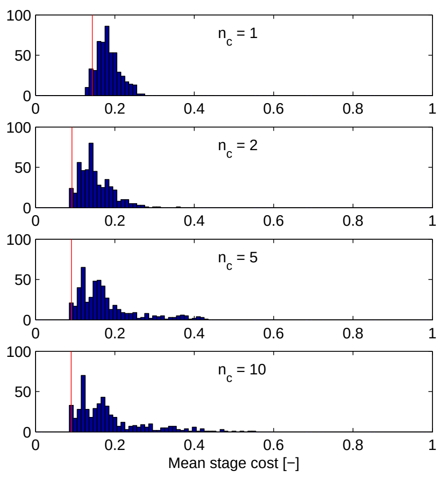

(b) System D

Figure 5.4: Histogram of mean stage cost. Red line shows cost with nominal system.

worst performance. The larger control horizon settings (2, 5 and 10) provided better control in terms of mean stage cost.

Any improvements to robustness in terms of control quality were not observed. The range of mean stage cost remained approximately the same for all the systems.

Chapter 6

Conclusion

In the first chapter, we presented the basic idea behind model based predictive control, briefly reviewed history of MPC and finally, the state of the art was shown.

In the second chapter, the most important components of predictive controller were described. Receding horizon concept was presented and simple constraints were illustrated. Then, elementary implementations of the regulator problem, the reference tracking problem and offset-free tracking were shown. It was also shown that the optimization problem arising in MPC is a quadratic program.

The third chapter dealt with quadratic programming, which is a minimization of quadratic function. First, quadratic program was defined, and conditions for it to be convex were stated. Then, quadratic programs were divided into three groups according to the type of constraints and several algorithms to solve each of them were presented.

For the unconstrained quadratic programs, two gradient methods and Newton's method were presented. Equality constrained QPs can be solved through the solution of the KKT system. Finally, active set method, fast gradient method and interior point method for the solution of inequality constrained quadratic programs were shown.

The fourth chapter addressed the first part of the assignment, i.e. the properties of QP algorithms and computation time distribution. In order to do this, several solvers representing each algorithm class were selected. Then, a simple benchmark control problem was chosen to deploy MPC controller and to run the simulation with the examined solvers. Finally, the solvers were tested with randomly generated bound constrained quadratic programs.

The influence of optimization problem size, condition number and the number of active constraints in optimum on the computation time was illustrated. The following relations were observed during the experiments.

The computation time is highly affected by the number of variables. Active set method exhibits quite strong dependence of computation time on the number of active constraints in the optimum. Computation time of fast gradient method strongly depends on the condition number and for ill-conditioned problems it depends on the number of active constraints as well. The larger the condition number, the slower the rate of convergence. Interior point method keeps the computation time almost constant irrespectively of the number of active constraints and condition number.

The fifth chapter addressed the second part of the assignment. The chapter presented the robustness of unconstrained MPC controller in terms of control performance. First, the influence of individual model parameters inaccuracy was shown. Then, the effect of MPC control horizon length on the control quality was studied.

It was demonstrated that there is a need for an exact model of a system. In case of system-model mismatch, the control quality is poor, unless special care is taken such as disturbance estimation through an observer. For all the systems, no improvement to robustness was observed with increasing control horizon.

Generally, it is a good idea to set control horizon long enough. For the simple second order systems from Section 5.2, control horizon set to two gave almost the same control performance as five and ten did. This is good to know, because the shorter control horizon dramatically decreases optimization problem complexity. However, control horizon set to one gave much worse control performance.

The only difference was the system with unstable zero. The control performance was roughly the same for all the control horizon settings. This is probably due to the fact that the tracking error was dominated by the negative response caused by the zero. Surprisingly, for a system with unmodelled time delay, longer control horizon may lead to poor tracking because the system oscillates.

Both tasks given in the assignment were accomplished. However, there are still many open questions to deal with. Here, only two of them are pointed out. First, there are many more QP algorithms to study. Several approaches that combine the properties of the algorithms dealt in this thesis exist that give great performance in MPC. Second, different cost functions can be used in MPC, which leads to different optimization tasks and therefore to different approaches to the solution.

Bibliography

[1] J. A. Rossiter, *Model-based predicitve control: a practical approach.* CRC Press LLC, 2003.

[2] J. Richalet, A. Rault, and J. Testud, "Algorithmic control of industrial processes," in *Proceedings of the 4th IFAC symposium on identification and system parameter estimation*, pp. 1119–1167, 1976.

[3] C. R. Cutler and B. L. Ramaker, "Dynamic matrix control - a computer control algorithm," in *Proceedings of the joint automatic control conference*, 1980.

[4] J. Rawlings, "Tutorial overview of model predictive control," *Control Systems, IEEE*, 2000.

[5] S. J. Qin and T. A. Badgwell, "A survey of industrial model predictive control technology," vol. 11, pp. 733–764, 2003.

[6] H. J. Ferreau, P. Ortner, P. Langthaler, L. D. Re, and M. Diehl, "Predictive control of a real-world Diesel engine using an extended online active set strategy," *Annual Reviews in Control*, vol. 31, pp. 293–301, Jan. 2007.

[7] S. Richter, C. N. Jones, and M. Morari, "Real-time input-constrained MPC using fast gradient methods," *Proceedings of the 48h IEEE Conference on Decision and Control (CDC) held jointly with 2009 28th Chinese Control Conference*, pp. 7387–7393, Dec. 2009.

[8] Y. Wang and S. Boyd, "Fast Model Predictive Control Using Online Optimization," *IEEE Transactions on Control Systems Technology*, vol. 18, pp. 267–278, Mar. 2010.

[9] S. Richter, S. Mariethoz, and M. Morari, "High-speed online MPC based on a fast gradient method applied to power converter control," in *American Control Conference (ACC), 2010*, pp. 4737–4743, 2010.

[10] K. Basterretxea and K. Benkrid, "Embedded high-speed Model Predictive Controller on a FPGA," *2011 NASA/ESA Conference on Adaptive Hardware and Systems (AHS)*, pp. 327–335, June 2011.

[11] F. Borrelli, A. Bemporad, and M. Morari, "Predictive Control for linear and hybrid systems," 2011.

[12] G. Valencia-Palomo, M. Pelegrinis, J. A. Rossiter, and R. Gondhalekar, "A move-blocking strategy to improve tracking in predictive control," *American Control . . .*, pp. 6293–6298, 2010.

[13] A. Bemporad, M. Morari, V. Dua, and E. N. Pistikopoulos, "The explicit linear quadratic regulator for constrained systems," *Automatica*, vol. 38, pp. 3–20, Jan. 2002.

[14] O. Šantin, *Influence of Model Uncertainty on Constraints Handling in Predictive Control.* Diploma thesis, CTU in Prague, 2009.

[15] G. Franklin, J. D. Powell, and A. Emami-Naeini, *Feedback control of dynamic systems.* Pearson, 2010.

[16] B. Grünbaum, *Convex polytopes.* New York: Springer, 2nd ed., 2003.

[17] J. Nocedal and S. J. Wright, *Numerical Optimization.* New York: Springer, second ed., 2006.

[18] S. Boyd and L. Vandenberghe, *Convex Optimization.* Cambridge University Press, seventh ed., 2004.

[19] Y. Nesterov, *Introductory Lectures on Convex Optimization: A basic Course.* Kluwer Academic Publishers, 2004.

[20] M. Knapp-Cordes and B. McKeeman, "Improvements to tic and toc Functions for Measuring Absolute Elapsed Time Performance in MATLAB," *MATLAB Digest*, pp. 1–4, 2011.

[21] M. Hoč, *Helicopter in virtual space.* Diploma thesis, CTU in Prague, 2008.

[22] D. P. Bertsekas, "On the Goldstein - Levitin - Polyak Gradient Projection Method," *IEEE Transactions on Automatic Control*, vol. AC-21, no. 2, pp. 174–183, 1976.

[23] A. Bemporad and M. Morari, "Robust model predictive control: A survey," *Robustness in identification and control*, 1999.

[24] U. Maeder and M. Morari, "Offset-free reference tracking with model predictive control," *Automatica*, vol. 46, pp. 1469–1476, Sept. 2010.

[25] A. S. Badwe, R. S. Patwardhan, S. L. Shah, S. C. Patwardhan, and R. D. Gudi, "Quantifying the impact of model-plant mismatch on controller performance," *Journal of Process Control*, vol. 20, pp. 408–425, Apr. 2010.

[26] J. L. Garriga, M. Soroush, and H. M. Soroush, "On the Effects of Tunable Parameters of Model Predictive Control on the Locations of Closed-Loop Eigenvalues," *Industrial & Engineering Chemistry Research*, vol. 49, pp. 7951–7956, Sept. 2010.

Appendix A

Contents of the attached CD

The attached CD contains two directories:

thesis: Full text of the thesis in Portable Document File.

program: Source codes for MPC controller simulation and QP algorithms from Chapter 3. Several examples of MPC simulation and QP solution are included as well. Matlab installation is required.